Fundamental Characteristics and Applications of an Inductively

Coupled Plasma as an Ion Source for Mass Spectrometry

by

Jeffrey Scott Crain

PHD Thesis submitted to Iowa State University

Ames Laboratory, U.S. DOE

Iowa State University

Ames, Iowa 50011

Date Transmitted: January 1990

MASTER

Fundamental characteristics and applications of an inductively

coupled plasma as an ion source for mass spectrometry[1]

Jeffrey Scott Crain

In charge of major work: R.S. Houk
From the Department of Chemistry
Iowa State University

Noise power spectra of the $^{85}Rb^+$ signal and the $^{93}Nb^+$ signal from an inductively coupled plasma-mass spectrometer were compared to the noise power spectrum of Sr II emission from the plasma. Discrete frequency noise in the emission at the mass spectrometer sampling orifice was found to be nearly identical to that in the mass spectrometer signal. However, discrete frequency noise in emission from the plasma alone differed substantially in frequency from that in the mass spectrometer signal. The dependence of noise frequencies on plasma operating conditions was generally the same for the mass spectrometric measurements and both emission measurements. These results indicate that the plasma was the source of discrete frequency noise in the mass spectrometric signal. The major source of signal instability in this particular ICP-mass spectrometer was found to be 1/f noise.

A new, home-made ICP-mass spectrometer was used to study the influence of Na, K, and U on ion signals from Y, Co, and As. In general, analyte signals were suppressed in the presence of excess matrix element. The extent of suppression was greatest for the element with high ionization energy (As) and least for the element with the smallest ionization energy (Y). These trends in the interference effect could be altered by applying a positive voltage to the first element of the ion optics. When the skimmer orifice diameter was made smaller than the sampling orifice diameter, analyte signal suppression was uniform and more extensive. Under these conditions, the heavy matrix element (U) induced more suppression than did the light matrix element (Na).

Degrees of ionization for As and Sb in an inductively coupled plasma were measured using mass spectrometry, and electron density (n_e) in the plasma just upstream of the mass spectrometer sampling orifice was measured from Stark broadening of the H I 486.13 nm emission line. These data were used to calculate ionization temperature (T_{ion}) for Sb and As over the range of plasma conditions studied. Variations of Sb T_{ion} with plasma conditions were consistent with those expected of the ICP itself, however, such was not always the case for As T_{ion}. It was found that T_{ion} for Sb was generally higher than that of As, indicating that the ionization kinetics of Sb may differ from those of As.

Fundamental characteristics and applications of an inductively

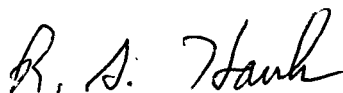coupled plasma as an ion source for mass spectrometry

by

Jeffrey Scott Crain

A Dissertation Submitted to the

Graduate Faculty in Partial Fulfillment of the

Requirements for the Degree of

DOCTOR OF PHILOSOPHY

Department: Chemistry
Major: Analytical Chemistry

Approved:

In Charge of Major Work

For the Major Department

For the Graduate College

Iowa State University
Ames, Iowa

1989

TABLE OF CONTENTS

1

GENERAL INTRODUCTION

Inductively coupled plasma-mass spectrometry (ICP-MS) is an

instrumental technique for trace elemental and isotopic analysis.

Instruments designed for ICP-MS consist of an inductively coupled plasma

ion source, an atmospheric pressure sampling interface, and typically, a

quadrupole mass spectrometer. The prototype ICP-MS instrument was

designed and constructed at Iowa State University in the late 1970s by

R.S. Houk and co-workers (1,2). Further research and development in the

United States, Canada, and England (3-20) preceded commercial production

of these instruments by Sciex (Thornhill, Ontario, Canada) and VG

Elemental (Winsford, Cheshire, England) in 1983. Initially, industrial

acceptance of ICP-MS as a viable technique for elemental analysis was

withheld, due largely to early studies indicating poor instrumental

stability (21-27) and severe interelement interferences (24,28-35).

Thus, in its infancy, the technique gained its foothold in academic and

governmental circles. Further development led to modifications in

instrumental design, which in turn led to improved instrumental

performance, especially in the area of long-term instrument stability.

In addition, investigators have reported a variety of novel applications

for ICP-MS, including stable isotope tracing of human and animal mineral

metabolism (36-42) and element-selective detection for chromatography

(43-47). The combination of these factors has led to a surge in the

production and sale of these instruments over the past 2 years, such

that ICP-MS has been listed among the "hot" scientific research areas

world-wide, along with such topics as AIDS and high temperature

superconductivity (48).

In principle, ICP-MS instruments are relatively simple to understand. Atoms, ions and electrons present in the ICP flow through a small (ca. 1 mm diameter) orifice drilled into a metal sampling cone, and enter a sampling chamber held at approximately 1 torr by a suitable mechanical vacuum pump. The flow rate of particles through the sampling orifice is governed by the temperature of the ICP in the sampled plasma volume, the size of the sampling orifice, and the pressure ratio across the sampling orifice, i.e., the ratio of atmospheric pressure to that inside the sampling chamber (49-51). Inside the sampling chamber, the sampled particles form a jet expansion, the dimensions of which are determined by the same factors that govern particle flow through the sampling orifice. A conical "skimmer", mounted coaxially and downstream of the sampler, collects a fraction of the jet expansion. The efficiency of the skimming process, i.e., the relative size of the fraction removed from the jet expansion, is determined by the geometry of the skimmer cone, the position of the cone relative to the sampling orifice, and the size of the skimmer orifice (49-53). Ions contained in the "skimmed" fraction are collected and focused by electrostatic ion optics and are conducted into the mass analyzer where the ions are separated on the basis of different mass-to-charge ratios. Detection of the mass-analyzed ions is accomplished with a suitable particle detector, e.g., an electron multiplier operated in a positive ion mode.

As stated earlier, ICP-MS instruments are fairly simple to understand in principle. However, this statement should not be taken to mean that useful analytical data are simple to obtain from ICP-mass

spectrometers. In practice, useful analytical results are only obtained when careful consideration is given to details in design, construction and operating conditions such that ions are produced, sampled, transmitted, and detected optimally. However, even under such constraints, there are fundamental physical limitations imposed upon the optimum ability of the instrument to produce and detect ions. Some of these limitations can be inferred from the description already given. For example, it is readily apparent that the sampling efficiency of the instrument is limited by the sampled plasma volume and the fraction of the jet expansion taken into the mass spectrometer by the skimmer, i.e., every ion produced in the ICP is not sampled and every ion sampled does not reach the mass spectrometer. Thus, even under optimal sampling conditions, a theoretical limit to sampling efficiency exists. This limitation has been described elsewhere (49,50). Additional factors such as space-charge limited ion transmission (51,54), mass analyzer resolution, and dynamic range limitations of the detector (27,55) also contribute to the overall efficiency of the instrument. Such limitations could be overcome by substantial changes in instrument design. However, the description of such modifications is beyond the scope of the present work. In fact, with the number of ICP-mass spectrometers installed world-wide (approximately 250 instruments as of this writing), sweeping changes in instrumental design would be somewhat impractical at this point in the evolution of the technique. Thus, investigation of the limitations imposed upon the method by the existing instrumentation should have a greater impact upon the field.

The purpose of this dissertation is to describe instrumental noise properties and matrix interferences characteristic of current ICP-mass spectrometer design. From this information, practical solutions to these problems can be suggested. Furthermore, this dissertation also describes the application of ICP-MS to fundamental plasma characterization, which is an area that has received limited study to date. Each of these topics is presented in an individual section of this dissertation. Each section stands independent of the others as a complete scientific manuscript with figures, tables and literature cited. Additional literature cited in this introduction and in the summary following the last section will be given after the summary.

The first section describes the noise characteristics of the output signal from an ICP-mass spectrometer. These measurements were unique for two reasons. First, this important instrumental property had not yet been investigated by any other workers in the field. Second, these measurements were multidimensional in that optical noise measurements from Sr II emission upstream of the ICP-MS sampling cone were directly compared to simultaneous mass spectrometric noise measurements. Thus, this study not only allowed estimation of instrumental contributions to signal instability in ICP-MS, but also permitted isolation of the various instrumental sources of this instability and estimation of their contribution to the whole.

The second section of this dissertation describes the interference of NaCl, KCl and $UO_2(NO_3)_2$ sample matrices upon the analytical signal of Co, As and Y from an ICP-mass spectrometer. The variation of these interferences with sampling interface geometry and ion optical voltage

is also presented, and a mechanism for these interferences, based on the properties of the supersonic expansion and sampling interface geometry, is proposed which qualitatively explains some of the observed trends.

The third and final section of this dissertation presents the results of ionization temperature calculations for the ICP using optical measurement of electron density upstream of the ICP-MS sampling interface and simultaneous mass spectrometric measurement of degrees of ionization for As and Sb. The variation of ionization temperature for these elements with ICP operating conditions is described, and observations of interelement differences in ionization temperature are reported. A comparison is made between ionization temperatures measured on a "home-made" ICP-mass spectrometer and those measured on a commercially available ICP-MS instrument, and differences found in this comparison are reported.

SECTION I.

NOISE POWER SPECTRAL CHARACTERISTICS OF AN INDUCTIVELY COUPLED

PLASMA-MASS SPECTROMETER

Introduction

Since the advent of inductively coupled plasma-mass spectrometry

(ICP-MS) in the late 1970s, investigators have found many valuable

applications of this technique. Among these applications are trace

elemental and isotopic analysis of geological materials (1-5), stable

isotope tracing of metabolic pathways in living organisms (6,7), and

trace elemental analysis by isotope dilution (8-10). However, there is

general agreement that the precision achievable by ICP-MS stands in need

of improvement. For example, isotope ratios measured by ICP-MS have

relative standard deviations (RSDs) ranging between 0.3% and 1.0% for

commercially available instruments. However, the exceptional precision

of thermal ionization mass spectrometry (typically 0.01% RSD) makes it

the technique of choice when small isotope ratios or small isotope

enrichments are to be measured and when sample throughput is not a

consideration. Houk and Thompson (11) have discussed the factors

limiting the precision of ICP-MS isotope ratios, and, based upon the

findings of other workers (6-8,12-14), have concluded that the precision

of isotope ratios measured by ICP-MS is primarily limited by

instrumental stability. Currently, the signal stability of commercially

available ICP-mass spectrometers is around 5% RSD over a period of

several hours. A logical step in the advancement of ICP-MS as a

technique for elemental and isotopic analysis is to improve these figures for stability and precision. Therefore, the sources of instrumental noise in an ICP-mass spectrometer should be isolated and characterized, such that the deleterious effects of instrumental noise on measurement precision can be minimized.

To date, no studies of ICP-MS noise power spectral characteristics have appeared in the literature. However, a number of investigators have reported studies of noise power for the ICP as an optical emission source (15-19). These studies have found that, in general, the noise power spectral characteristics of ICP emission depend on plasma operating parameters and torch design. Belchamber and Horlick (16) showed that discrete frequency noise in ICP emission could be attributed to the rotation of an asymmetric plasma, but Winge et al. (19) have proposed an alternate mechanism for discrete frequency noise production involving the vortex ring phenomenon (20). In the present work, no attempt is made to elucidate the mechanisms by which noise is produced in the ICP-mass spectrometer. However, comparisons between mass spectral noise and optical noise from both the emission of the ICP alone and emission of the ICP during sampling for mass spectrometry are made, and preliminary connections are drawn between the three.

Experimental

Instrumentation

The ICP-mass spectrometer used in this study has been described previously (21). The detector assembly used in these experiments was modified from that used in the earlier design. This new assembly is shown in Figure 1. In this new assembly, the scintillator detector was
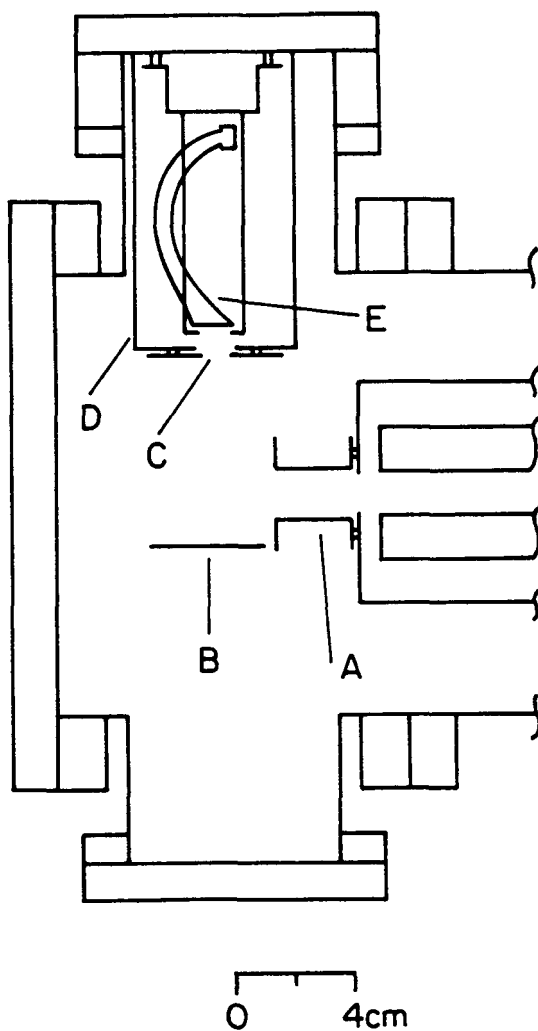
Figure 1.   ICP-MS detector assembly. (A) quadrupole exit lens, (B) ion reflecting plate, (C) detector housing aperture, (D) multiplier housing, (E) Channeltron electron multiplier

9

Table 1. Instrumental Components

Component Manufacturer/Description	Operating Conditions

nebulizer
  cross flow with Scott double
  pass spray chamber (22) and
  desolvation apparatus (23)
 peristaltic pump:
 Minipuls 2
 Gilson Medical Electronics
	desolvation temperature: 140 °C
	solution uptake: 2.5 mL min^{-1}

ICP torch and generator (22)
  load coil grounded at turn
  closest to sampler (24)
	argon flow rates (L min^{-1}),
	except where noted in text:
	  outer: 15.6
	  aerosol: 1.0
	  auxiliary: only used during ICP
	        startup ·
	forward power, except where noted
	in text: 1.4 kW
	reflected power: <5 W

ion extraction interface (21,25)	sampling position, except where noted in text: on center, 10 mm above top of coil sampler orifice diameter: 0.79 mm skimmer orifice diameter: 1.6 mm skimmer-sampler separation: 8 mm operating pressure: 1.1 torr

ion optics (21)	applied voltages:
	  first cylindrical lens: -149
	  photon baffle: -10
	  second cylindrical lens: +34
	  third " " : -169
	  fourth " " : -149
	  differential pumping orifice: -90
	  ELFS lens: -90

mass analyzer
  model 270-9 with
  model 012-14 RF head
  Extranuclear Laboratories
  (now Extrel)
	rod bias (V): +1
	FWHM resolution at m/z 85: 98

Table 1.   (continued)

Component Manufacturer/Description	Operating Conditions

detector assembly
  Ames Laboratory construction
  (see Figure 1)
	applied voltages:
	    quadrupole exit lens: -290
	    ion deflecting plate: +800
	    detector housing aperture: -1250

detector
  Channeltron electron multiplier
  model 4830A
  Galileo Electro-optics Corp.
	operating voltage: -3 kV
	approximate gain = 10^7

detector output conversion
  current-to-frequency converter
  model 151
  Analog Technologies Inc.
	sensitivity: 10^{-12} A Hz^{-1}

multichannel analyzer:
  model 66 with 20 MHz dual-
  input multichannel scaler
  Nuclear Data Inc.
	dwell time/channel: 500 µs
	channels: 4096

spectrum analyzer
  model 3582A
  Hewlett-Packard
	acquisition rate: 2 kHz
	bandpass: uniform
	bandwidth: 4 Hz
	sensitivity: varied with operating
	            conditions to prevent
	            input overloading.

monochromator
  model 8200
  Jarrell-Ash division
  (now Thermo Jarrell-Ash)
	Ebert mount
	focal length: 0.5 m
	grating: 1160 grooves mm^{-1} blazed
	        at 250 nm.
	exit slit: 10 mm long X 25 µm wide
	entrance slit: same dimensions as
	              exit, masked to 1 mm
	              height.

photomultiplier
  model R955
  Thorn EMI
	applied voltage: -700 V

replaced by a Channeltron electron multiplier offset 90° from the center line of the quadrupole mass analyzer. An ion deflecting plate, aligned with the mouth of the electron multiplier, was placed below the cylindrical exit lens of the mass analyzer such that ions exiting the quadrupole were steered into the entrance aperture in the detector housing. The voltages applied to the ion optical elements in this assembly are given in Table 1. A detector assembly having similar geometry and components has been described previously (25).

Data acquisition

The operating conditions and components of this instrument are described in Table 1. A schematic diagram of the experimental apparatus is shown in Figure 2. In the mass spectrometric experiments, ion signals for $^{85}Rb^+$ and $^{93}Nb^+$ were measured by nebulizing a solution of Rb and Nb, each at 1 mg L^{-1}. The kinetic energy distribution of $^{93}Nb^+$ was measured by the electrostatic retardation method described previously (24,26) after each change in plasma operating conditions.

For emission studies, a pyrex lens (5 cm diameter, f/2) was used to focus an image of the plasma (magnification 1.4) on the entrance slit of a monochromator. The monochromator was turned so that the entrance slit was parallel to the ICP torch, and the slit was masked to a height of 1 mm. The monochromator and photomultiplier (PMT) used in this study are described in Table 1 and have been used in a previous study (27). Optical emission measurements were made by nebulizing a solution of Sr at 4 mg L^{-1} and monitoring the signal arising from the Sr II line at 407.7 nm.
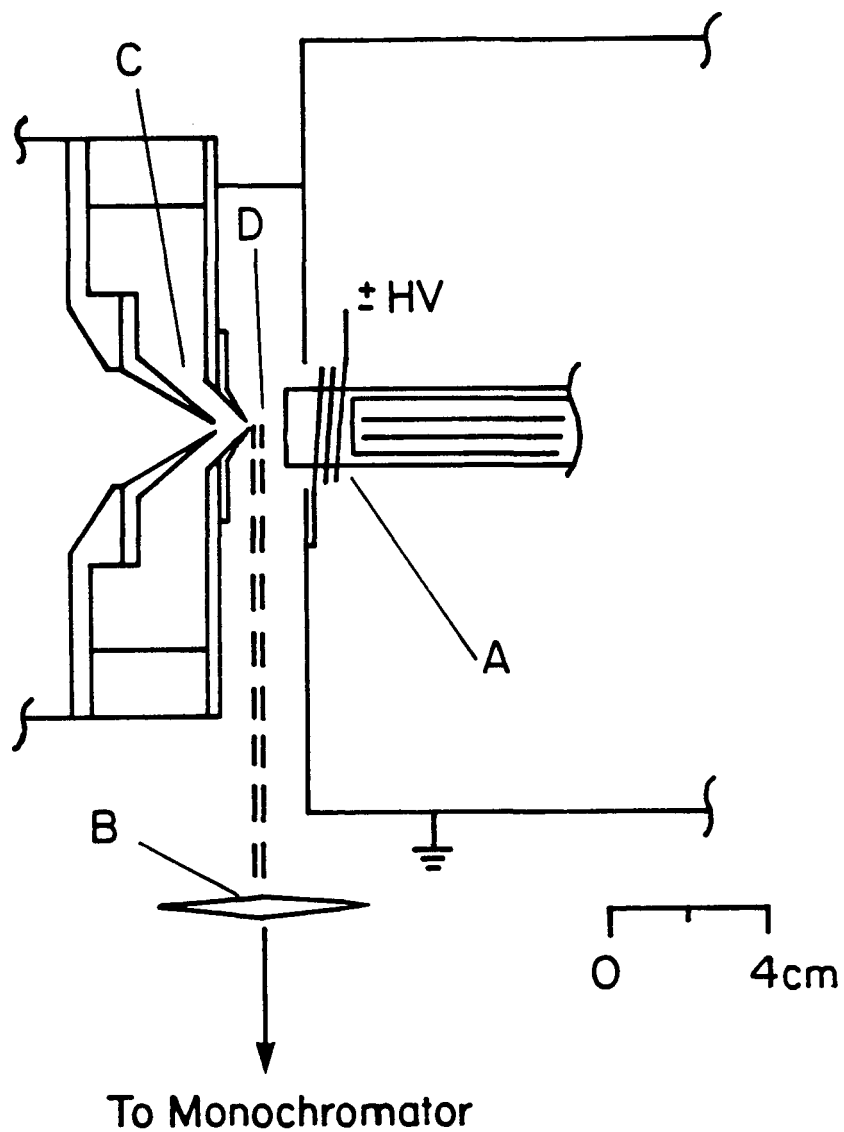
Figure 2. Spatial arrangement of (A) ICP torch, (B) lens, (C) ion
extraction interface, and (D) region viewed by
monochromator. Monochromator not shown

Noise power spectra were obtained by one of two methods. In the first of these methods, a 512-point frequency spectrum analyzer was connected directly to the output of the channeltron electron multiplier. With the quadrupole mass spectrometer transmitting the analyte m/z of interest, the current output of the channeltron was read by the spectrum analyzer and Fourier transformed. A similar procedure was used to obtain noise power data from the optical emission using a photomultiplier and monochromator. Adequate noise power data were obtained in the mass spectrometric experiments when 64 transforms were averaged, but an average of 128 transforms was used in the optical emission experiments. Examples of noise power spectra taken by this method can be found in Figures 3b and 3c. This method offered the significant advantage of direct noise power measurement during experiments. However, because the measurement bandwidth of the spectrum analyzer was chosen to be 4 Hz, the actual frequency at which a fluctuation occurred could be within ± 2 Hz of that measured. For example, a fluctuation in signal appearing as a noise peak at 400 Hz may have a real frequency between 398 and 402 Hz.

An alternate method for obtaining noise power data involved the use of a current-to-frequency converter. This device was connected to the output of the detector and the train of TTL pulses output by the converter was carried to the input of a multichannel analyzer. The number of pulses in the train were counted by the analyzer for a specified dwell period and these data were stored in the appropriate memory channel of the device. The data collected after each time scan of the analyzer were transferred to a floppy disk, permitting the

14

storage of 23 4096-point scans. A method for converting these data into a noise power spectrum has been described (19). Figure 3a shows an example of noise power spectra collected by this method. The advantage of this method was higher frequency accuracy, owing to the chosen bandwidth of 0.5 Hz, than that obtained with the spectrum analyzer. However, the multichannel analyzer method required considerable data processing after data collection, and thus, was far slower than the spectrum analyzer.

Results and Discussion

General observations

Using the methods described above, noise power spectra from the ICP optical emission and ICP-mass spectrometer were taken at various plasma operating conditions corresponding to points on and around the maximum of the ICP-MS parameter behavior plot (28,29). Noise power data were acquired at a rate of 2 kHz, yielding frequency spectra in the range 0 to 1 kHz. No noise peaks were observed at frequencies exceeding 1 kHz. Acquisition of noise power data at 4 kHz and 10 kHz gave no indications of aliasing in the resultant noise spectra. A battery providing a dc current of comparable magnitude to the detector output was connected to the input of the measuring device. Using this arrangement, it was found that the white noise in either measurement system was < -90 dB.

In general, the noise power spectra measured by the multichannel analyzer method exhibited white noise levels between -55 dB and -70 dB. The white noise in the signal from the mass spectrometer was 5 to 10 dB higher than that present in the optical emission signal. Narrow peaks were present in the spectra which corresponded to pickup of 60 Hz noise

and its harmonics from surrounding power lines. These spectra also showed the low frequency $1/f$ noise profile typical of nebulizer noise and instrumental drift (16). Spectra acquired early in the course of these experiments exhibited noise peaks at 9 Hz, 18 Hz, and occasionally at 27 Hz. The frequencies of these peaks did not change with operating conditions. Using a stroboscopic tachometer (model GR1538-A, GenRad, Concord, MA) it was found that these frequencies corresponded to the rotational frequency of the rotors in two of the belt-driven mechanical pumps used with the vacuum system. Thus, vibrations caused by these pumps caused the signal instability at these frequencies. Replacement of these pumps with vibrationally quiet or vibrationally isolated pumps eliminated these peaks from the noise power spectra.

Finally, the spectra also exhibited peaks at higher frequency (above 120 Hz) which did not correspond to harmonics of the power line frequency and varied in frequency with variations in ICP operating conditions. In general, the intensities of these peaks were roughly 5 to 10 dB higher than the white noise. However, because the bandpass characteristics of the spectrum analyzer were chosen so as to favor simple frequency measurement rather than intensity measurement, these intensities could not be measured precisely. The frequencies of these peaks in the ICP-MS noise power spectra were independent of analyte mass, i.e., the frequencies did not change for various ions studied in the m/z range between $^{14}N^{+}$ and $^{175}Lu^{+}$. The properties of these peaks are discussed in the next two sections.

Comparison of noise from emission and mass spectrometry

Figure 3 compares the noise power spectra of the ion signal from $^{85}Rb^+$ to that of the Sr II 407.7 nm emission under identical plasma operating conditions. Note that Figure 3a was acquired by the current-to-frequency conversion method described above, whereas Figures 3b and 3c were acquired with the spectrum analyzer. The differences in the white noise characteristics of the three spectra are immediately obvious but not immediately explicable. However, if the vertical scale of Figure 3a is expanded by a factor of 4, it can be shown that the white noise in that figure decreases in a way similar to that shown in Figures 3b and 3c, i.e., from -65 dB at 0 Hz to -68 dB at 1 kHz. The source of this decrease in white noise is not certain, but may arise from the variable frequency response of the low pass or "anti-aliasing" filtering function present in the multichannel analyzer method (19), and, to a lesser degree, also present in the spectrum analyzer. However, it is also possible that this effect is real, i.e., the 1/f noise "tail" is of sufficient length and intensity to cause the "background" noise (normally only white noise) to decrease with increasing frequency.

Figure 3a shows the noise power spectrum of emission from the ICP alone, i.e., the ICP was not being sampled for mass spectrometry. The observation position relative to the end of the torch was the same as that shown in Figure 2 except that the plasma, lens and monochromator were moved back from the sampling orifice as a unit such that the ICP no longer came into contact with the sampler. The dominant peak in the spectrum is found at 283 Hz and appears to be a harmonic of 142 Hz, which is also found in the spectrum. Figure 3b shows the noise power
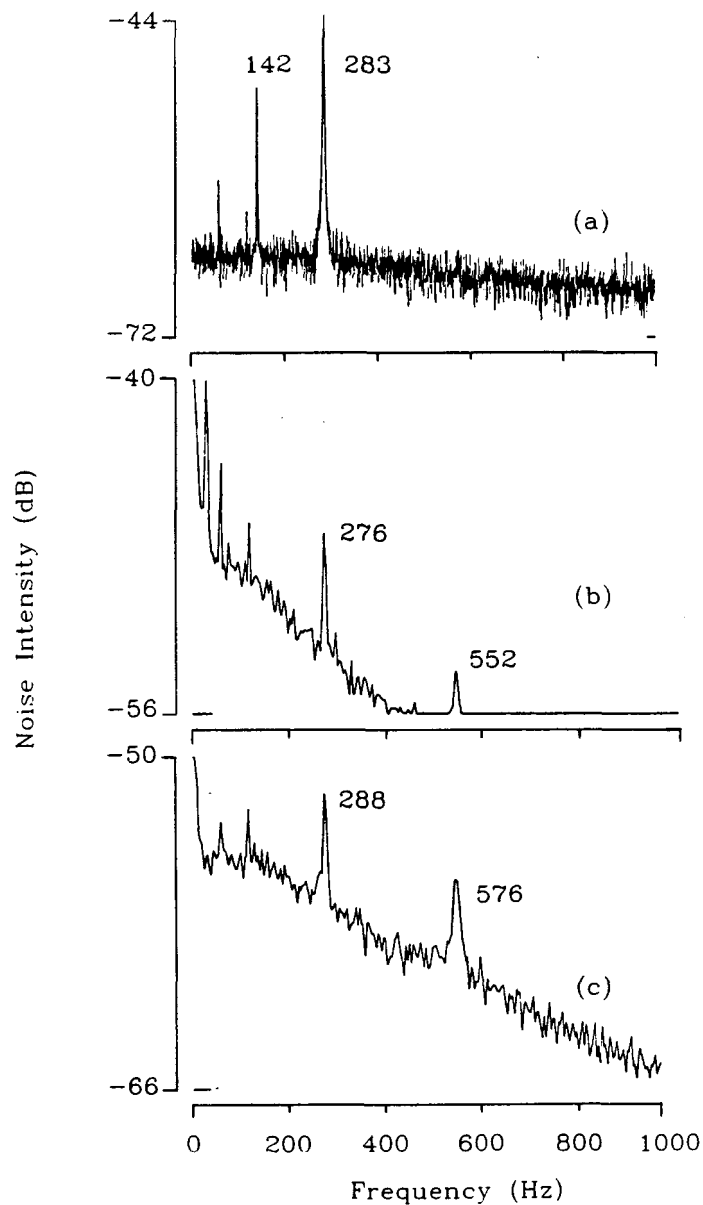
17

Figure 3. Comparison between noise power spectra from (a) ICP
emission, (b) ICP emission upstream of the ICP-MS
sampler, and (c) the ICP-mass spectrometer. ICP outer
gas flow 15.5 L min^{-1}, otherwise, plasma conditions as
given in Table 1. Numbers on these and subsequent
figures represent peak frequencies

spectrum from ICP emission when the ICP was being sampled for mass spectrometry. Note that the frequencies of the peaks have shifted to 276 Hz and 552 Hz. These "shifted" frequencies are close to those seen in Figure 3c, the noise power spectrum from the ICP-mass spectrometer.

In general, comparison of noise power spectra from ICP emission in front of the ICP-MS sampling orifice (Figure 3b) to noise power spectra from the ICP-mass spectrometer under identical plasma operating conditions showed that discrete frequency noise in the optical emission occurred at slightly lower frequency than that observed in the mass spectrometer signal. This difference probably arose from the differences in sampling between the two experiments, i.e., due to the width and height of the monochromator entrance and the diameter of the ICP-MS sampling orifice, photons and ions were sampled from slightly different parts of the ICP. Further comparisons between noise power spectra of the ICP-mass spectrometer under the same operating conditions on different days showed that the relative error in reproducing noise frequencies on the spectrum analyzer from day-to-day was ± 3%, due in part to the 4 Hz bandwidth of the spectrum analyzer as well as slight day-to-day errors in reproducing plasma position and operating conditions.

It is readily apparent that noise power spectra from the ICP-mass spectrometer and ICP emission during ICP-MS sampling are substantially different from the noise power spectrum of emission from the ICP alone. It is possible that the plasma noise source undergoes a substantial physical change during the ICP-MS sampling process, thereby changing the fundamental noise frequency. However, the frequencies observed in

Figures 3b and 3c closely correspond to the frequencies of the second

and fourth harmonics of the 142 Hz fundamental observed in Figure 3a,

i.e., 283 Hz and 576 Hz. Thus, it may also be possible that the

sampling process in ICP-MS does not change the plasma noise source, but

simply amplifies different harmonics of the fundamental noise frequency

from those amplified in the ICP alone. Further fundamental study of ICP

noise sources should make it possible to determine which of the

mechanisms described above is most feasible.

Dependence of noise frequencies on plasma operating conditions

Figure 4 shows the variation of peak frequency with ICP forward

power for the noise power spectrum of the $^{93}Nb^+$ signal from the mass

spectrometer. These spectra were obtained in rapid succession using the

spectrum analyzer by decreasing the power in increments of 100 W while

holding all other conditions constant. Table 2 shows the dependence of

the $^{93}Nb^+$ kinetic energy on ICP forward power. Figure 4a shows the

noise power spectrum at 1.4 kW. The peaks in the spectrum appeared at

284 Hz and 568 Hz. The frequencies of these peaks decreased at 1.3 kW

forward power, as shown in Figure 4b, and decreased further at 1.2 kW,

as shown in Figure 4c. Thus, the noise frequency of the mass

spectrometric signal decreased as ICP forward power decreased.

This is a real trend, not an artifact of the measurement technique,

because the differences in frequencies of the fundamental peaks (268

284 Hz) just exceed the bandwidth of the spectrum analyzer. Thus, the

frequencies of the peaks at 284, 276 and 268 Hz are definitely

distinguishable. Furthermore, the differences in frequency between the

harmonics above 500 Hz far exceed the 4 Hz bandwidth of the spectrum
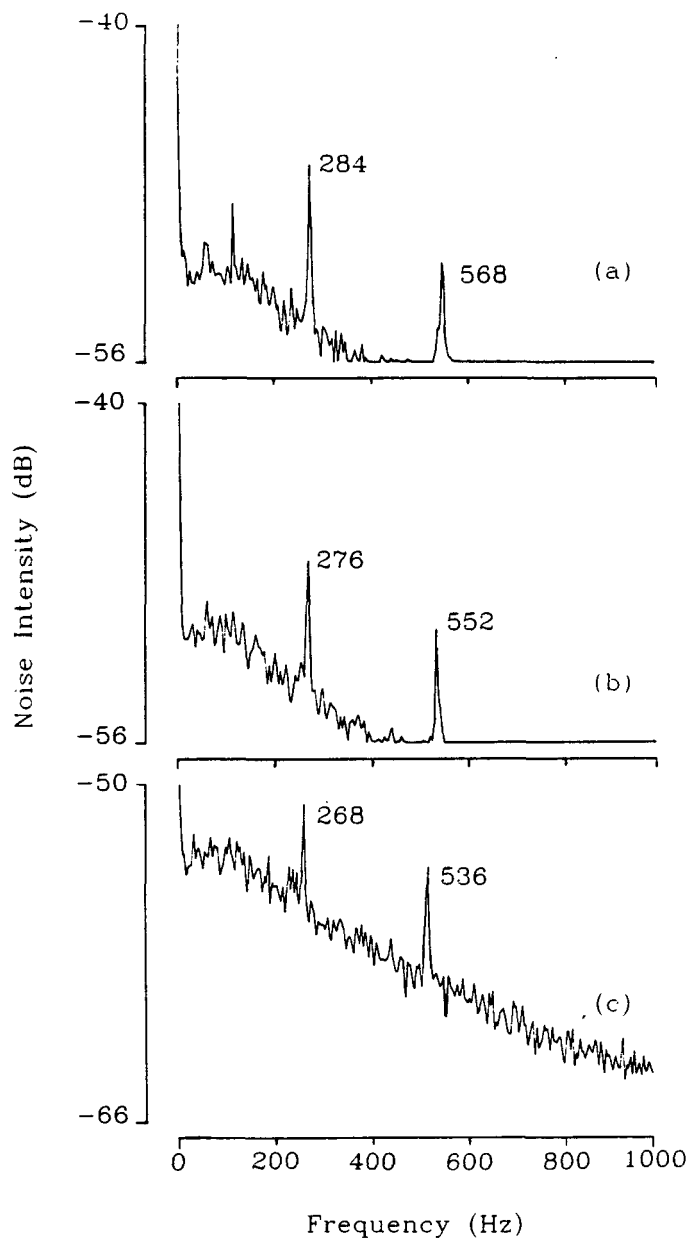
Figure 4. Variation of ICP-MS noise power spectra with ICP forward
power. (a) 1.4 kW, (b) 1.3 kW, (c) 1.2 kW. Other plasma
conditions given in Table 1

Table 2. Influence of ICP-MS Operating Parameters on Analyte Ion

Kinetic Energy

Power (kW)	Ion Kinetic Energies (eV) at Indicated Aerosol Gas Flow Rates[a]			
	0.9 L min^{-1}	1.0	1.1	1.2
1.2	-	10 eV	-	-
1.3	8.1 ± 0.2[b]	8.5	10.6	> 15
1.4	8.0	7.9	8.6	13.3
1.5	-	7.6	-	-

[a]The entries in this table represent the energy at which 90% of the $^{93}Nb^+$ signal was attenuated (26).

[b]Typical range of these measurements.

analyzer. This decrease in noise frequency with decreasing forward power was also observed in the noise power spectra of the ICP emission measurements taken during this study, and has been reported in prior noise power studies of emission from the ICP alone (16,19).

Figure 5 shows the dependence of noise frequency in the mass spectrometer signal on the ICP outer gas flow rate. These spectra were obtained in much the same way as those shown in Figure 4, although the $^{85}Rb^+$ signal was monitored in this experiment. Figure 5a shows the noise power spectrum at an outer gas flow rate of 16 L min^{-1}. Two peaks were found which decreased in frequency when the flow rate was decreased to 15.5 L min^{-1}, as shown in Figure 5b. The noise power spectra from ICP emission upstream of the ICP-MS sampling orifice showed peaks at the same frequencies as those shown in Figures 5a and 5b under the same plasma conditions. At 15 L min^{-1}, an extremely large peak appears in the noise power spectrum at 484 Hz along with a smaller peak at 544 Hz, as shown in Figure 5c. These peaks and an additional peak at 244 Hz were found in the noise power spectrum of ICP emission upstream of the sampling orifice at the same plasma conditions. It is probable that the peak at 244 Hz is a lower order harmonic of the 484 Hz peak and simply was not intense enough to appear in the ICP-MS noise power spectrum.

Based on the sharp frequency drop between the 576 Hz peak in Figure 5b and the 484 Hz peak in Figure 5c, as well as the presence of the 544 Hz peak in Figure 5c which more closely fits the apparent overall trend toward gradual frequency decreases, it is possible that the 484 Hz peak and its harmonic arise from a noise source different from that which produced the peaks in Figures 5a and 5b. However, regardless of the
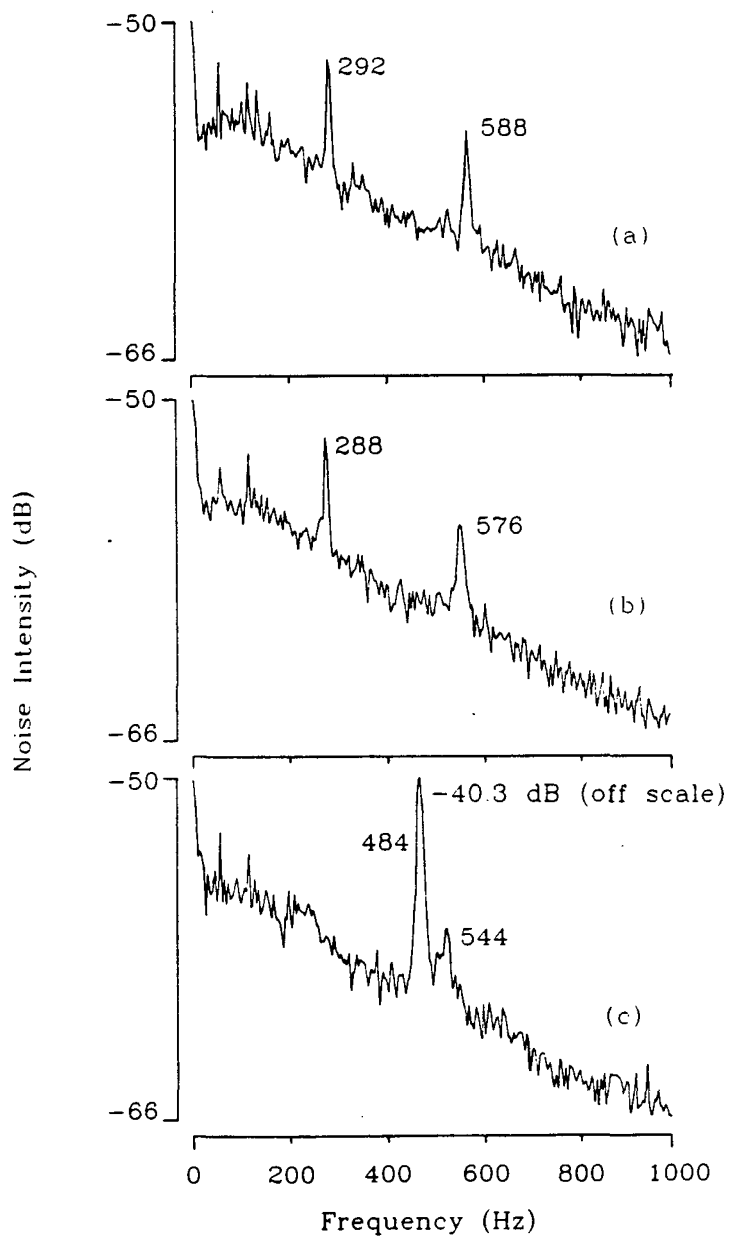
Figure 5. Variation of ICP-MS noise power spectra with ICP outer
gas flow rate. (a) 16 L min^{-1}, (b) 15.5 L min^{-1}, (c) 15
L min^{-1}. Other plasma conditions given in Table 1

noise source at 15 L min^{-1}, the observed trend between noise frequency
and outer gas flow rate in ICP-MS and ICP emission upstream of the
sampler has also been reported in previous studies of the ICP alone (16-
19). It would be useful to determine the effect of still lower outer
gas flow rates on the 484 Hz peak, however, these measurements were not
made because the walls of the ICP torch overheated at the 15 L min^{-1}
outer gas flow rate.

Figure 6 shows the variation in noise frequency in the $^{93}Nb^+$ signal
with variation in the axial position of the ICP relative to the tip of
the sampler. The spectra shown were acquired in much the same way as
those shown in Figure 4. Figure 6a shows the ICP-MS noise power
spectrum at 10 mm downstream from the top turn of the load coil, which
was 3 mm from the tip of the initial radiation zone in the ICP (30). As
shown in Figures 6b and 6c, the noise peaks decreased in frequency when
the axial position of the ICP was increased to 12 mm and then to 14 mm.
The audible noise emanating from the sampling interface (i.e., a
"whine") also decreased in pitch as the plasma was translated further
from the sampler. Therefore, a trend toward lower noise frequency at
larger axial sampling position clearly exists in this ICP-mass
spectrometer. Previous noise power studies of ICP emission reported no
dependence of noise frequency on observation height (18,19).

For comparative purposes, noise power spectra of ICP emission were
taken during ICP-MS sampling under various operating conditions at ICP-
MS sampling positions of 10 mm and 18 mm. In both cases, photons from
Sr II 407.7 nm emission were sampled from a region of the plasma 0.7 mm
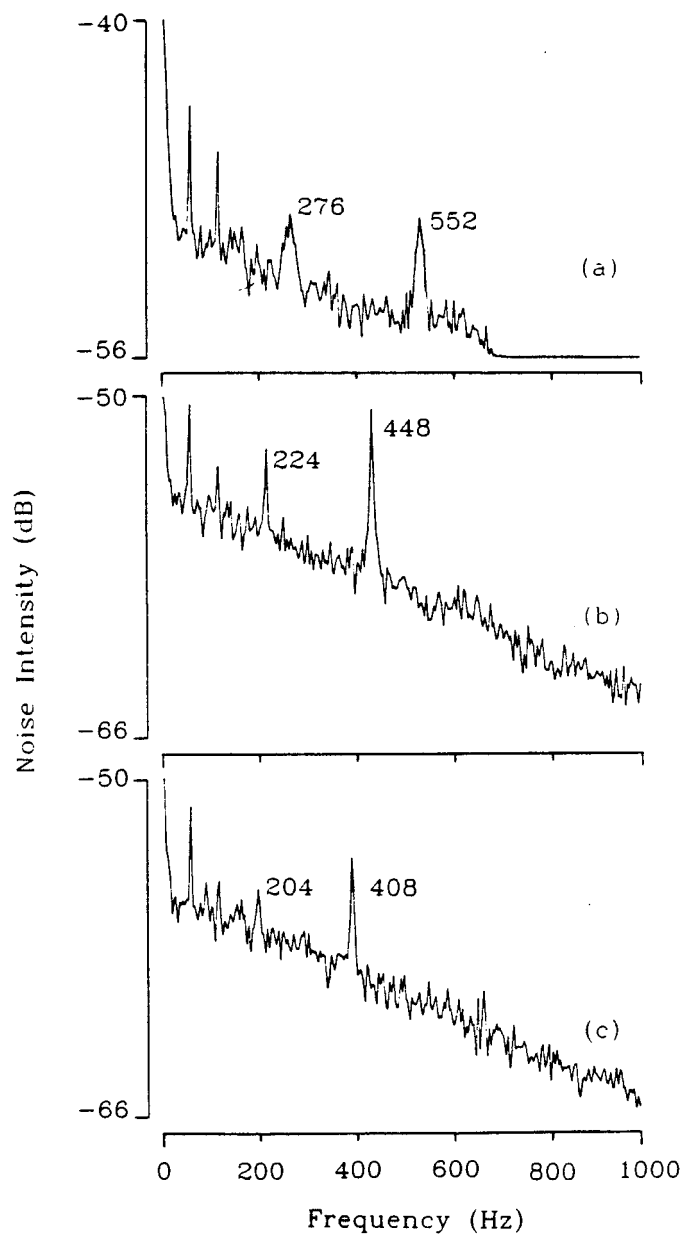long and 18 μm wide which began 1 mm upstream of the ICP-MS sampling

Figure 6. Variation of ICP-MS noise power spectra with load coil-
sampler separation. (a) 10 mm, (b) 12 mm, (c) 14 mm.
Other plasma conditions given in Table 1

orifice. Figure 3b shows the emission noise power spectrum measured 10 mm downstream of the load coil, while Figure 7 shows the noise power spectrum measured at 18 mm. It should be noted that the noise frequencies in this spectrum are identical to those shown in Figure 6a, which are from the mass spectrometer at the same plasma conditions. Translating the plasma back to 18 mm, as shown in Figure 7, caused an increase in the noise frequencies with a concurrent amplification of the dominant low frequency peak. This trend is entirely different from those described above for ICP-MS and ICP emission, leading to the conclusion that the observed trends in each experiment probably arise from different phenomena. The amplification of the dominant peak as shown in Figure 7 has also been reported in the ICP noise power studies of Winge et al. (19), which may evidence a physical connection between these phenomena, even though they lead to different frequency-position relationships.

The variation in ICP-MS noise frequency with aerosol gas flow rate were also measured. The spectra were acquired in much the same manner as those shown in Figure 4. The frequency of noise peaks did not change as aerosol gas flow rate was varied in the range between 1.0 and 1.2 L min^{-1}. Thus, there is no apparent dependence of noise frequency on aerosol gas flow rate in ICP-MS over the range of aerosol gas flow rates studied. This experiment was repeated at a different ICP forward power (1.3 kW). The frequency of the noise peaks decreased as expected from the forward power-frequency dependence described above (see Figure 3), but these noise frequencies did not change when the aerosol gas flow rate was changed. The noise frequencies were also independent of
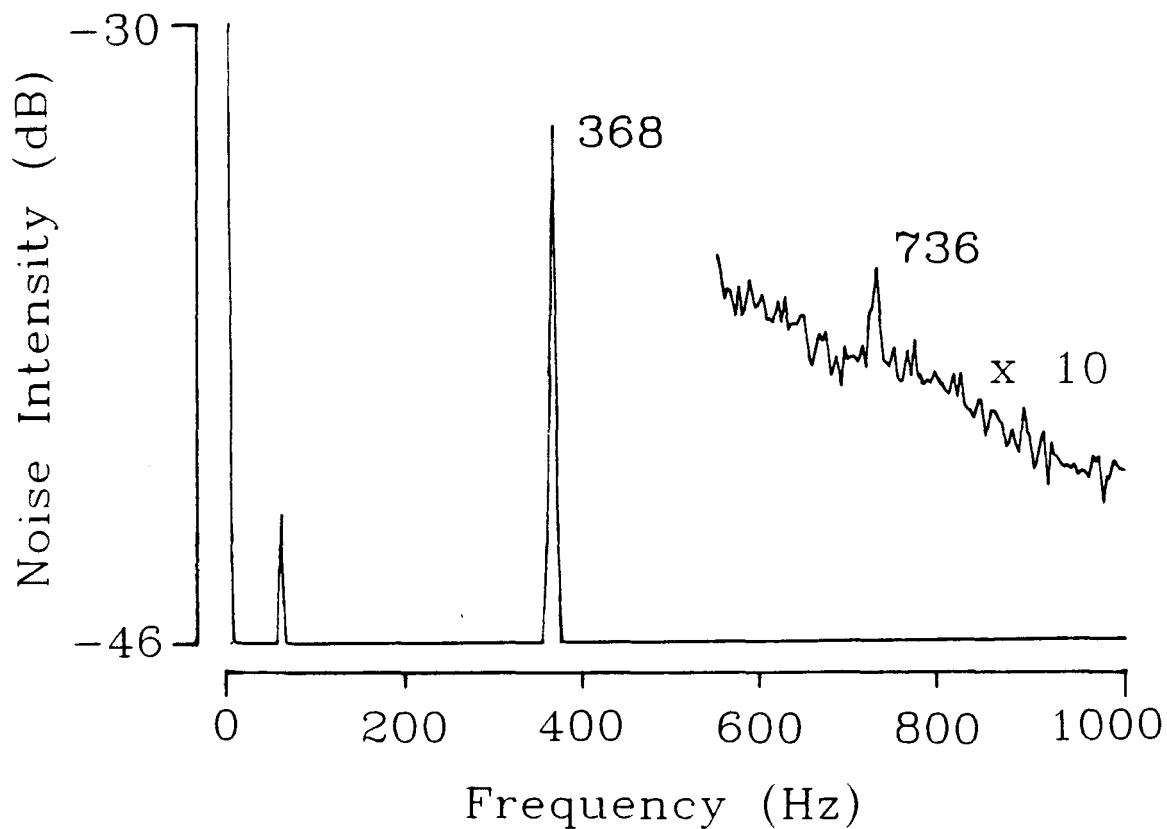
Figure 7. Noise power spectrum from ICP emission upstream of the
ICP-MS sampling orifice at an 18 mm load coil-sampler
separation. ICP outer gas flow 15.5 L min^{-1}, otherwise,
plasma conditions as given in Table 1

aerosol gas flow rate for ICP emission upstream of the ICP-MS sampler and for the noise power spectra of emission from the ICP alone. This independence has been observed in previous noise studies of ICP emission (16,19).

Table 2 shows the kinetic energy of ions inside this ICP-MS device under various plasma operating conditions. When plasma conditions were altered to cause an increase in ion kinetic energy, the noise power spectra of the signal from these higher energy ions were, for all practical purposes, identical to the noise power spectra of photon emission from ions just upstream of the sampling cone. Thus, it would appear that the mild residual discharge upstream of the sampling orifice in this "homemade" ICP-MS instrument (24,26,31), which is thought to influence ion kinetic energy, affects emission noise and mass spectrometer noise in the same manner.

It is also important to note that the dependence of noise frequency on various plasma parameters closely follows that of emission from the ICP alone, with the important exception of the frequency-axial position dependence (Figure 6). This different behavior can be justified as follows. Changing observation height in an ICP emission experiment merely involves translating the plasma or the viewing optics. The plasma itself is not altered during this positioning process. However, changing the sampling position in an ICP-MS experiment involves translating the plasma relative to the fixed, solid sampling cone. The cone is actually immersed in the plasma such that gas from the center of the ICP flows through the sampling orifice, and the rest of the plasma is deflected by the outer surface of the sampling cone. Because the

plasma makes physical contact with the sampler, it is reasonable that inserting the sampler into the plasma can affect the gas dynamics of the ICP. Therefore, if discrete frequency noise in signals coming from the axial channel of the ICP actually has its origins in the outer gas flow as has been proposed (16,19), then moving the ICP relative to the stationary sampler would perturb the dynamics of gas flow in and around the interface, such that noise frequency would change as well.

Relative contributions of various noise sources in ICP-MS

It is also instructive to compare the relative magnitudes of the various noise sources and their individual contributions to the stability of the ICP-MS signal. The RSD (in %) of a measured signal can be calculated from the noise level N (in dB) using the equation:

$$RSD \approx 10^{2+(N/20)} \tag{1}$$

In the present work, white noise levels of -55 to -60 dB were observed for ion currents which, based on a detector gain of 10^7, would yield an approximate counting signal of 10^6 ions s^{-1}. Using equation 1 and the white noise levels above, white noise as the sole noise source would be expected to yield RSDs of 0.1 to 0.2%. These RSDs are comparable to those expected from counting statistics for the ion count rate given. This level of precision also corresponds roughly to the best precision obtainable on occasions when isotope ratios are measured using fast scanning or rapid peak hopping, such that the contributions of 1/f noise and discrete frequency noise are minimized. However, isotope ratio measurements are generally less precise than counting statistics would predict (11,21,32). Thus, it is apparent that the other noise sources must contribute to the poorer precision of these measurements.

During single ion monitoring, the overall signal stability for this particular ICP-mass spectrometer with a Channeltron detector is typically 5% RSD at a sampling rate of 2 kHz and a 2 s integration time. Thus, white noise, although higher than in ICP emission, is a minor contributor to the overall instability in the signal, based on the above calculation. The remaining noise must therefore originate from a superposition of 1/f noise and discrete frequency noise. As discussed earlier, the relative magnitudes of these noise sources are difficult to estimate accurately, owing to the chosen measurement characteristics of the spectrum analyzer. However, a general, qualitative comparison between these noise sources can be justified by examining the maximum possible contribution to the overall noise based on the amplitude of the discrete frequency fluctuations. For example, as shown in Figure 5c, an intense 484 Hz fluctuation can be induced in the analytical signal of the mass spectrometer at the proper plasma conditions. Under these plasma conditions, if the noise contribution of this fluctuation were maximized by sampling the analytical signal at twice the frequency of the fluctuation, then this -40 dB fluctuation would yield a RSD of only 1%. Even this maximum contribution is small compared to the overall signal stability of 5% RSD. Thus, it is reasonable to conclude that, for the data acquisition conditions used in this work, the major contributor to the total signal instability in this ICP-mass spectrometer is 1/f noise.

Conclusions

The evidence presented in this study indicates that the primary source of discrete frequency noise in ICP-MS is the ICP itself. The differences between the noise frequencies in ICP emission and ICP-MS may be caused by gas dynamic interaction between the ICP and the mass spectrometer sampling cone. The similarity between the noise power spectra of ICP-MS signal and ICP emission signal at the sampler provides evidence for such a conclusion. However, this is not to say that the mass spectrometer does not contribute to ICP-MS stability. In fact, such factors as pump vibration and instability in ion transmission and detection will all contribute to the total noise of the ICP-MS instrument. The effect of these factors is evident in this study, since it would appear that for this particular instrument, 1/f noise is the major cause of signal instability. These noise sources may be attenuated by efficient vibrational isolation of the pumps from the vacuum system, better electronic control of the instrument, careful ion optical design and higher stability detectors. In fact, improvements in the thermal stability of the electronics and changes in ion optical design have been shown to improve the stability of commercial ICP-mass spectrometers (32). Furthermore, discrete frequency noise in ICP emission can be attenuated by using an extended tangential flow torch (19) or an extended laminar flow torch (18). Based on the findings given in the present work, measures such as these could substantially attenuate noise in the analytical signal of this ICP-mass spectrometer.

Literature Cited

1. Smith, R.G.; Brooker, E.J.; Douglas, D.J.; Quan, E.S.K.; Rosenblatt, G. J. Geochem. Explor. **1984**, 21, 385.

2. Gregoire, D.C. Anal. Chem. **1987**, 59, 2479.

3. Longerich, H.P.; Fryer, B.J.; Strong, D.F.; Kantipuly, C.J. Spectrochim. Acta, Part B **1987**, 42B, 75.

4. Date, A.R.; Cheung, Y.Y.; Stuart, M.E. Spectrochim. Acta, Part B **1987**, 42B, 3.

5. Gray, A.L. Analyst **1985**, 110, 551.

6. Serfass, R.E.; Thompson, J.J.; Houk, R.S. Anal. Chim Acta **1986**, 188, 73.

7. Janghorbani, M.; Ting, B.T.G.; Fomon, S.J. Am. J. Hematol. **1986**, 21, 277.

8. Dean, J.D.; Massey, R.; Ebdon, L.J. J. Anal. Atomic Spectrom. **1987**, 2, 369.

9. McLaren, J.W.; Beauchemin, D.; Berman, S.S. Anal. Chem. **1987**, 59, 610.

10. Hall, G.E.M.; Park, C.J.; Pelchat, J.C. J. Anal. Atomic Spectrom. **1987**, 2, 189.

11. Houk, R.S.; Thompson, J.J. Mass Spectrom. Rev. **1988**, 7, 425.

12. Russ, G.P. III; Bazan, J.M. Spectrochim. Acta, Part B **1987**, 42B, 49.

13. Longerich, H.P.; Fryer, B.J.; Strong, D.F. Spectrochim. Acta, Part B **1987**, 42B, 39.

14. Ting, B.T.G.; Janghorbani, M. Spectrochim. Acta, Part B **1987**, 42B, 21.

15. Walden, G.L., Bower, J.N.; Nikdel, S.; Bolton, D.L.; Winefordner, J.D. Spectrochim. Acta, Part B 1980, 35B, 535.

16. Belchamber, R.M.; Horlick, G. Spectrochim. Acta, Part B 1982, 37B, 17.

17. Davies, J.; Snook, R.D. J. Anal. Atomic Spectrom. 1986, 1, 195.

18. Davies, J.; Snook, R.D. J. Anal. Atomic Spectrom. 1987, 2, 27.

19. Winge, R.K.; Eckels, D.E.; DeKalb, E.L.; Fassel, V.A. J. Anal. Atomic Spectrom. 1988, 3, 849.

20. Van Dyke, M. "An Album of Fluid Motion"; The Parabolic Press: Stanford, CA, 1982.

21. Huang, L.-Q.; Jiang, S.-J.; Houk, R.S. Anal. Chem. 1987, 59, 2316.

22. Scott, R.H.; Fassel, V.A.; Knisely, R.N.; Nixon, D.E. Anal. Chem. 1974, 46, 75.

23. Houk, R.S.; Fassel, V.A.; LaFreniere, B.R. Appl. Spectrosc. 1986, 40, 94.

24. Olivares, J.A.; Houk, R.S. Appl. Spectrosc. 1985, 39, 1070.

25. Olivares, J.A.; Houk, R.S. Anal. Chem. 1985, 57, 2674.

26. Crain, J.S.; Houk, R.S.; Smith, F.G. Spectrochim. Acta, Part B 1988, 43B, 1355.

27. Houk, R.S.; Lim, H.B. Anal. Chem. 1986, 58, 3244.

28. Horlick, G.; Tan, S.H.; Vaughan, M.A.; Rose, C.A. Spectrochim. Acta, Part B 1985, 40B, 1555.

29. Vaughan, M.A.; Horlick, G.; Tan, S.H. J. Anal. Atomic Spectrom. 1987, 2, 765.

30. Koirtyohann, S.R.; Jones, J.S.; Yates, D.A. Anal. Chem. **1980**, 52, 1965.

31. Gray, A.L.; Houk, R.S.; Williams, J.G. J. Anal. Atomic Spectrom. **1987**, 2, 13.

32. Douglas, D.J. Can. J. Spectrosc. **1989**, 34, 38.

SECTION II.

MATRIX INTERFERENCES IN INDUCTIVELY COUPLED PLASMA-MASS SPECTROMETRY:

SOME EFFECTS OF SKIMMER ORIFICE DIAMETER AND ION LENS VOLTAGES

Introduction

Numerous investigators have reported that analyte ion signals in ICP-MS depend upon the identity and concentration of the matrix element(s) in the sample solution to a greater extent than generally seen in ICP atomic emission spectrometry (ICP-AES) (1-9). Although the interferences in ICP-MS often can be attenuated simply by diluting the sample, this remedy naturally compromises detection limits, and excellent detection limits are among the most attractive features of ICP-MS. Investigations into the fundamental phenomena causing such interference effects could help alleviate them and improve the suitability of ICP-MS for determining analyte elements at trace or ultratrace levels in the presence of much more abundant matrix elements.

It was initially expected that analyte ion signals would be suppressed in the presence of a matrix element, and the initial ICP-MS investigations reported such effects (1-3). Suppression of analyte signal has remained the general rule, although enhancements of analyte ion signals can be observed in some cases. Several workers have described comprehensive studies of the dependence of matrix effects on various parameters such as ICP operating conditions and the mass and ionization energies of the analyte and matrix elements (4-8). Several mechanisms have been proposed to explain certain aspects of the observed

matrix interferences. These postulates include diffusion effects in the plasma (7), space charge repulsions in the ion beam (9), and collisional effects and mass enrichment phenomena during the extraction process (5,8).

The majority of published experimental work on matrix effects has been performed with the Sciex ICP-MS device. The load coil geometry used with this device almost totally prevents any electrical discharge between the plasma and the sampling orifice (10-12). Alternatively, other load coil geometries can be used, for which a mild but not overly malignant discharge persists (13,14). These latter instruments, including the VG Plasmaquad and several "home-made" devices, also generally suffer from suppression of analyte signal by matrix elements (2,3,15). There has also been little work reported so far with either type of instrument as to whether the interference effect can be influenced by changes in the sampling interface or variations in ion optical conditions. The present work shows that variations in this effect can occur, at least for one particular ICP-MS device.

Experimental

Instrumentation

The ICP-MS instrument used in this study (Figure 1) was assembled in the Ames Laboratory. Instrumental components and operating conditions are listed in Table 1. The basic design principles are similar to those employed in the original Ames Laboratory device (16). For example, the geometry of the ICP load coil employed in this instrument is similar to that used in the original device. However, several modifications to the original design have been incorporated in
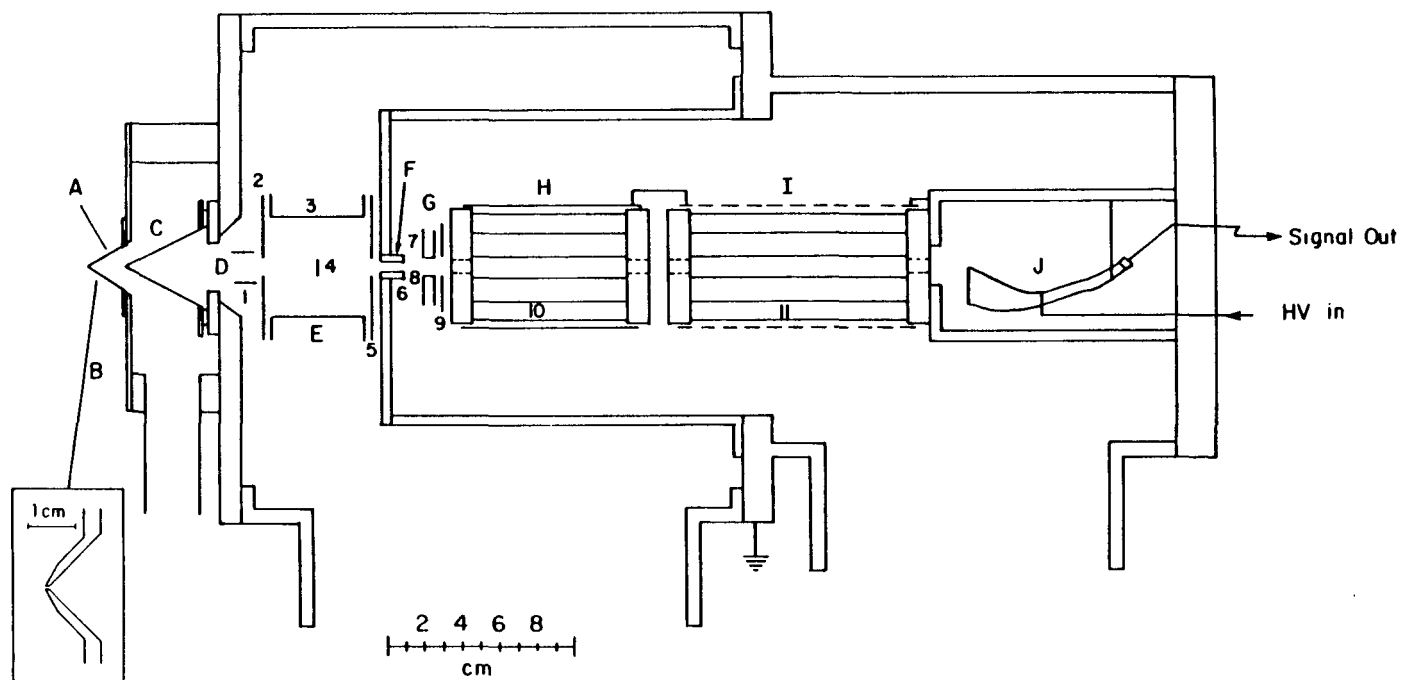
Figure 1. Diagram of ICP-MS used: (A) sampling cone; (B) water-cooled sampling flange;
(C) skimmer; (D) cylindrical ion lens; (E) Bessel box assembly; (F)
differential pumping orifice; (G) ion optics; (H) RF-only quadrupole and
solid RF shield; (I) quadrupole mass filter and wire mesh RF shield; (J)
Channeltron electron multiplier. The ICP equipment and nebulizer system are
not shown

38

Table 1. Instrumental Components

Component/Manufacturer	Operating Conditions

plasma generator
  type HFP-2500D with AMNPS-1
  impedance matching network
  RF Plasma Products, Inc.
  Kresson, NJ
 	
  load coil grounded at end
  nearest sampling orifice.
  See Figure 2x of ref. (13).
	forward power: 1.4 kW
	reflected power: < 10 W
	frequency: 27.12 MHz

plasma torch
  all quartz construction
  Ames Laboratory design (17)
  outer tube extended 20 mm
  beyond aerosol injector
	argon flow rates (L min^{-1})
	  outer: 13
	  aerosol: 0.9
	  auxiliary: 0.4

ultrasonic nebulizer power supply
  model UNPS-1
  RF Plasma Products, Inc.
	transducer power: 45 W

ultrasonic nebulizer
  mount, spray chamber, and
  desolvation apparatus:
  Ames Laboratory design
  (18,19)
	solution uptake rate: 2.9 mL min^{-1}
	desolvation temperature: > 100°C
	transducer frequency: 1.36 MHz
	transducer and condenser ice-water
	cooled

sampling position	15 mm from downstream turn of load coil. On center ca. 7 mm from tip of initial radiation zone (20).

vacuum system
  3-stage, differentially
  pumped, welded stainless
  steel construction, similar
  to ref. (16).
	first stage pressure 600 mtorr;
	second stage pressure 4 x 10^{-4} torr;
	third stage pressure 2.5 x 10^{-6} torr

Table 1.   (continued)

Component/Manufacturer	Operating Conditions

---

pressure measurement
  first stage

  second and third stage

Convectron thermocouple gauge
  series 275
  Granville-Phillips
ionization gauges
  model 843
  Varian

ion lens elements
  stainless steel construction
  Ames Laboratory design
  (see Figure 1)

voltage values: V_1= -12, V_2=-90,
  V_3= +20, V_4= -20, V_5= -60, V_6= -90
  V_7= -50, V_8= -40, V_9= -5, V_{10}= +5,
  V_{11}= +4

 quadrupole mass analyzer
  model 100C
  Uthe Technologies Inc.
  Sunnyvale, CA

RF-only rods mounted coaxially in
front of mass filter and operated
synchronously.

quadrupole control and power supply
  model 011-14
  Extranuclear Laboratories
  (now Extrel Inc.)
  Pittsburgh, PA

m/z scanned from 57 to 92
sweep driven by 0 to +10 V ramp
output from signal averager.

Channeltron electron multiplier
  model 4817
  Galileo Electro-Optics Corp.
  Sturbridge, MA

cathode bias = -2.8 kV,
gain: 10^7, anode electrically
isolated from channel.

detector mounting chamber
  model 051-72
  Extranuclear Laboratories

detector output measurement
  current-to-frequency converter
  model 151
  Analog Technology Corp.
  Pasadena, CA

sensitivity: 0.01 pA/Hz

signal averaging and readout
  model 1170
  Nicolet Instrument Co.
  Madison, WI

4096 channels per sweep
dwell time: 40 μs per channel
128 sweeps stored in memory

---

the new instrument. The expansion chamber of this device was larger than that previously used and was evacuated through two ports, each with its own rotary pump. The additional pumping speed gained in this manner permitted the use of larger orifices in the sampler, skimmer, and differential pumping plate. A large Bessel box (E, Figure 1) was incorporated in the ion optical assembly. The central photon stop and both end plates on the Bessel box were electrically isolated from each other and from the outer cylinder; each lens element was biased independently. An RF-only quadrupole (H) was incorporated for other experiments. For this study, it was simply used as an ion lens to conduct ions into the mass analyzer.

Analyte solutions were ultrasonically nebulized and desolvated prior to their introduction into the ICP (18,19). Atoms and ions produced in the ICP were extracted into the expansion chamber through a conical nickel sampler, which is shown in the inset of Figure 1. The orifice diameter (D_0) was 0.89 mm and the thickness of nickel at the very tip of the cone was approximately 1 mm. The internal and external angles of the sampler cone were 90 and 120°, respectively.

One of two stainless steel skimmers (C, Figure 1), denoted by a and b in the subsequent text, were used to extract ions from the jet expansion downstream of the sampler. Both skimmers had the same height (4.1 cm) and cone angles (50° internal, 60° external). Skimmer a had an orifice diameter (D_s) of 1.7 mm, whereas skimmer b had an orifice diameter of 0.76 mm. Because each skimmer was of equal height, the sampler-skimmer separation was the same (1.78 cm) for both, such that either skimmer would penetrate the Mach disk and sample the supersonic

expansion at the same position (16,21). The skimmer and sampler were both grounded to the vacuum system.

The same sampling orifice was used for all these studies. It was removed and cleaned after a complete interference curve was obtained for each matrix element. For Na and K, deposition was not extensive (22), and the orifice could be cleaned easily in an ultrasonically agitated water bath. After each experiment with uranium, the orifice was drilled out with a 0.89-mm diameter bit and then cleaned in the ultrasonic water bath. Once a cleaned sampler was remounted, the analyte ion sensitivity (i.e., ion current per mg L^{-1} in solution) could be recovered to within 5% from day to day.

Solutions

Stock solutions of Na and K were volumetrically prepared by dissolving reagent grade NaCl and KCl in doubly-deionized water. A uranium stock solution was prepared in the same manner from a stock solution of purified $UO_2(NO_3)_2$. Solutions having the desired salt concentrations were prepared by adding the appropriate volume of matrix stock solution with Co, As and Y standards so as to contain 1.0 mg L^{-1} of each analyte upon dilution. A "no-matrix" standard was prepared in the same fashion, without the matrix stock solution. Blank solutions of each matrix were prepared at the maximum concentrations used in the interference measurements.

Experimental method

Instrumental parameters (e.g., aerosol gas flow rate, power, and ion lens voltages) were chosen to yield maximum signal and minimum noise for 1 mg L^{-1} Co. Thus, all data reported below were taken at the

aerosol gas flow rate corresponding to the peak in the parameter

behavior plot for Co (8,23,24). Ion currents for Co, As, and Y were

obtained by measuring the net peak height of each ion from the signal

averaged mass spectrum of the analyte solution. In the absence of

interferent, the signal for the three monoisotopic analytes at 1 mg L^{-1}

was the order of 20-40 nA while the background was 30 ± 4 pA.

The "normalized signals" plotted in the figures below represented

the ratio of analyte signal in the presence of interferent to that in

the absence of interferent. Based on the precision of the analyte

intensities, the relative standard deviation (RSD) of each normalized

signal point was ± 7%. A set of such measurements for a range of

interferent concentrations constituted an interference curve. The

procedure for measuring the interference curve was the same as that

employed in an earlier study (3) except that the solutions were

nebulized continuously in the present work, i.e., flow injection was not

used. Blank solutions of each salt yielded no significant analyte peaks

or other isobaric interferences with Co, As, or Y in the concentration

range of interest, i.e., $ArCl^+$ was negligible compared to the signal for

As.

Ion currents for Cs and I from a 7.7 x 10^{-6} M deionized water

solution of CsI were collected following the completion of each

interference curve. Ionization temperatures were estimated from these

data using the ion current ratio of Cs to I (25) and an arbitrary

electron number density of 5 x 10^{14} cm^{-3} (26). The partition functions

were calculated from the compilation of de Galan et al. (27).

Results and Discussion

Interference measurements

Interference curves for 1 mg L^{-1} Co, As and Y in NaCl, KCl and

UO$_2$(NO$_3$)$_2$ were measured using skimmer a, under the plasma and ion

optical parameters listed in Table 1. These data are shown in Figure 2.

Analyte signal was lost as salt concentration increased above 3 x 10^{-3} M

and the extent of signal attenuation generally followed the order of

analyte ionization energies, i.e., Y (6.38 eV) was suppressed less than

Co (7.86 eV), which was in turn suppressed less than As (9.81 eV).

Breaks in the smooth descent of the curve at salt concentrations

exceeding 5 x 10^{-3} M were occasionally caused by incomplete rinsing

after analysis of a salt solution, leaving residual salt in the

nebulizer spray chamber. This residual salt suppressed the analyte

signal from the subsequent analysis of the deionized water reference

solution, thereby causing a positive error in the normalized signal.

This error was most pronounced for As, which was especially sensitive to

the presence of salts, as shown in Figure 2.

For each analyte, the molar concentration of salt that induced a

given amount of suppression increased in the order KCl < UO$_2$(NO$_3$)$_2$ $\leq$

NaCl. This trend did not follow the trend of interferent ionization

energy (K < Na < U) or interferent mass (Na < K << U). The trend

described above closely followed the order of T$_{ion}$ measured on the day

each of the suppression curves was obtained, as shown in Table 2.

Therefore, the small variation in the extent of interference induced by

different matrix elements may be attributed to the different T$_{ion}$ values

measured on the different days the experiments were performed.
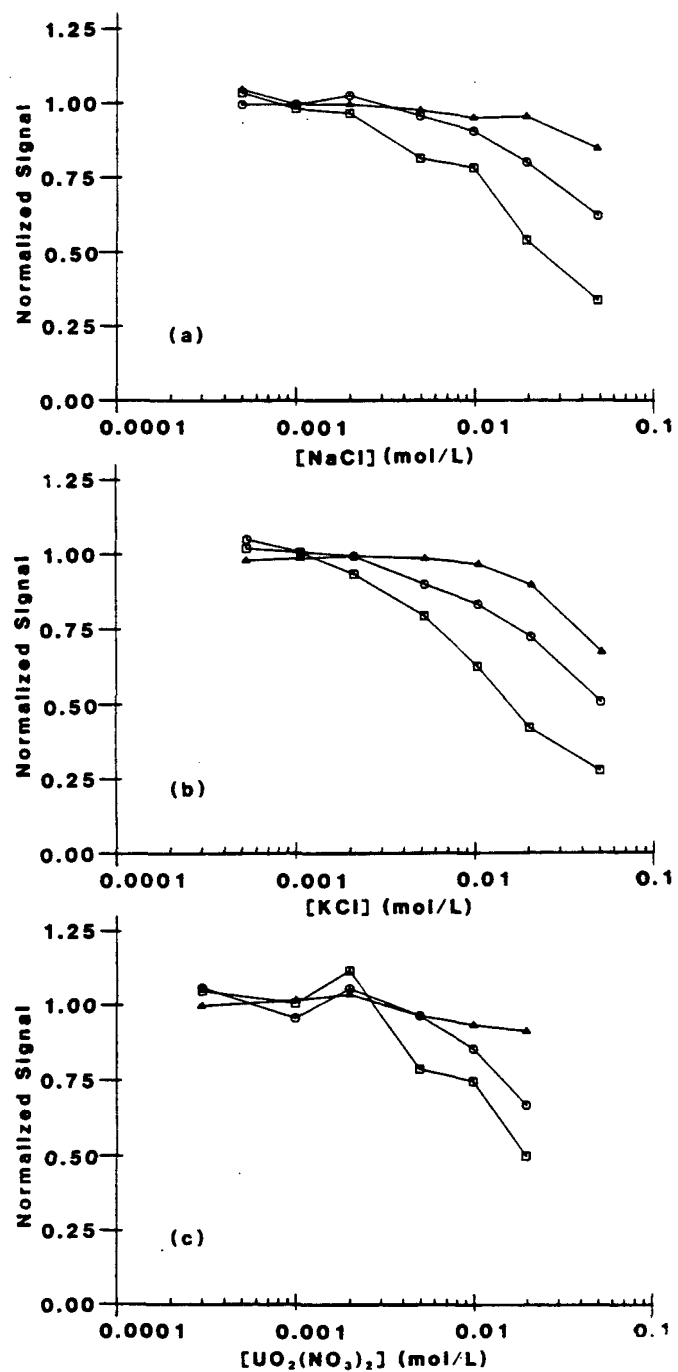
Figure 2.   Suppression of various analyte signals by (a) NaCl; (b) KCl; (c) $UO_2(NO_3)_2$.   Co signal (○), As (□), Y (△)

Table 2. T_{ion} Measurements

Day[b]	Matrix salt	Measured ratio (Cs^+/I^+)	T_{ion}[a] (K)
1	NaCl	2.81	7330
2	KCl	4.50	7060
3	$UO_2(NO_3)_2$	3.39	7220

[a]Calculated at $n_e = 5 \times 10^{14}$ cm^{-3}.

[b]Experimental interference curves were obtained on different days because it was necessary to clean the sampler between experiments. These data apply to Figure 2 only.

The shapes of the interference curves and the general magnitude of the suppression effects shown in Figure 2 were quite similar to those reported previously for the original Ames Laboratory device (3). In the previous work, a model was described which predicted analyte ionization suppression due to the release of additional electrons during ionization of the matrix element. The shapes of the curves in Figure 2 and the trend of interference with ionization energy of analyte agree precisely with those predicted by this model, although the extent of the interference at a given matrix concentration was much greater than that predicted by the model. Furthermore, the interference curve for Na were similar to those reported by Kawaguchi et al. for Co, Y, and La analytes (15). However, the interference behavior shown in Figure 2 substantially differs from that seen with the Sciex instrument in that the heavy matrix element (U) did not suppress the analyte signal much more extensively than the lighter interfering elements (5,8). A possible reason for this difference is discussed in the next section.

Influence of skimmer orifice diameter

The instrument used in the work described above differs from commercial ICP-MS devices in that the skimmer orifice was bigger than the sampling orifice. To allow a better comparison between "home-made" and commercial instruments, interference curves for 1 mg L^{-1} Co, As and Y in NaCl and $UO_2(NO_3)_2$ were measured using skimmer b (with the 0.76 mm orifice) under the same plasma and ion optical conditions as those used for interference measurements with skimmer a (see Table 1). Thus, the sampler-skimmer geometry was made similar to that found in the commercial ICP-mass spectrometers. Substitution of the smaller skimmer

attenuated the analyte ion signal by a factor of 3, which was in approximate agreement with the factor of 4 expected from the square of the ratio of the two orifice diameters (21).

The interference curves obtained with the smaller skimmer orifice are shown in Figure 3. The onset of analyte signal suppression occurred at lower salt concentrations than for skimmer a (see Figure 2), and at low salt concentrations, the extent to which analyte signal was attenuated at a given concentration was not greatly different for the three analytes. At high concentrations of U, where the analyte recovery was only 10% or less, the extent to which analytes were suppressed followed the order of analyte ionization energies, i.e., Y < Co < As.

With skimmer a installed in the instrument, U caused slightly more extensive interference than did Na, which was attributed to differences in T_{ion} between interference measurements. However, with skimmer b, U caused considerably more interference than Na, even though T_{ion} was the same (6900 K) for both interference curves in Figure 3. Furthermore, the same ICP parameters and sampling position were used in each case, such that any mass-dependent effects in the ICP alone should have been constant. Thus, the heavy interferent induced greater signal interference than the light interferent. The observation of enhanced analyte interference by heavy matrix elements has also been reported for commercial ICP-mass spectrometers. A possible explanation for this phenomenon has been described by Gillson et al. (9), and Tan and Horlick (8), and can be applied to the present work as follows: In the supersonic jet formed downstream of the sampler, light ions are more easily scattered toward the outer edges of the jet than are heavy ions.
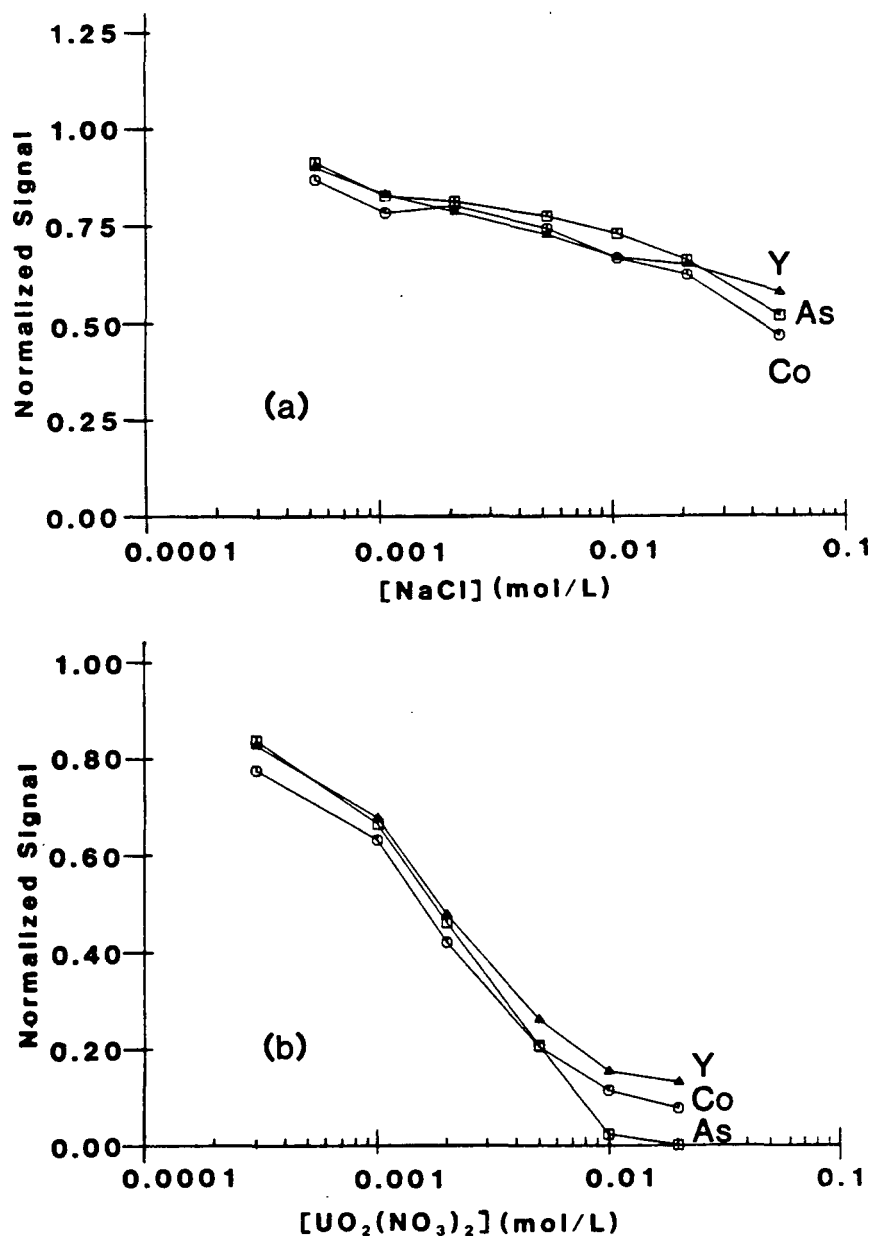
Figure 3. Suppression of signal for Co (○), As (□), and Y (△) by
(a) NaCl and (b) $UO_2(NO_3)_2$ using skimmer b (D_s= 0.76 mm)

Thus, heavy ions are enriched (relative to light ions) on the central axis of the supersonic expansion. This enrichment effect would be expected to increase as the skimmer orifice diameter decreases. If analyte ions are displaced by this enrichment phenomenon (8), or are scattered in the ion optics by space-charge repulsions due to matrix ion enrichment in the center of the jet (9), then smaller skimmer orifices would induce more extensive suppression effects because the density of a heavy matrix element (such as U) at the mouth of the skimmer would be higher than that of a light matrix element (e.g., Na). If this were the case, then a large skimmer orifice diameter would transmit a sufficient fraction of the jet through the skimmer such that enrichment effects would be minimal, and similar interference effects would be expected for all matrix elements, regardless of mass. This phenomenon is observed in Figure 2, where skimmer a (D_s = 1.7 mm) was used.

Effect of ion optical voltages

The previous interference curves were measured with the extraction cylinder (D, Figure 1) biased at -12 V (V_1, Table 1), which was the normal setting. Using skimmer a, interference measurements were also performed at other values of V_1. The voltage V_1 was decreased to -45 V without severe loss (i.e., < 30% reduction) of the analyte signal. This signal loss is primarily due to detuning of the ion beam at the extraction cylinder, since the other ion optical voltages were similar (often identical) to those listed in Table 1. Interference curves measured with V_1 in this negative range were very similar to those shown in Figure 2. Thus, changing V_1 in a negative direction did not affect the extent or the direction of the interference substantially.

Analogous experiments were also performed at V_1 = +2.5 V. This change increased the Co signal by approximately 30%, but the signal stability was considerably worse compared to the original ion optical conditions. Thus, a positive voltage on V_1 was not normally used with this device. The interference curves obtained with a positive voltage on the extraction cylinder are shown in Figure 4. Under these conditions, the analyte signal gradually decreased with increasing NaCl concentration. At low NaCl concentrations, the extent by which analyte signal decreased was not much different for the three analytes. However, at high NaCl concentrations, analytes were suppressed in the order Co ≈ As < Y, i.e., roughly the order of analyte mass rather than ionization energy.

An interesting aberration was observed one day during an attempt to duplicate the U interference curve at 2.5 V. This result is shown in Figure 5. In this situation, analyte signal was generally enhanced by the presence of $UO_2(NO_3)_2$ in the sample matrix up to a concentration of 10^{-2} M, at which point Co signal began to exhibit some suppression. At higher $UO_2(NO_3)_2$ concentrations, all analytes lost signal rapidly and were completely suppressed at a concentration of 2×10^{-2} M. This behavior was not attributable to radical differences in plasma conditions, since the measured T_{ion} for this experiment was only 100 K greater than that measured for the interference curve shown in Figure 4b. However, it was possible that variations in ion focusing characteristics between the two experiments contributed to the observed differences in analyte interference. Experimental measurements of apparent ion lens potential (i.e., the voltage measured across the

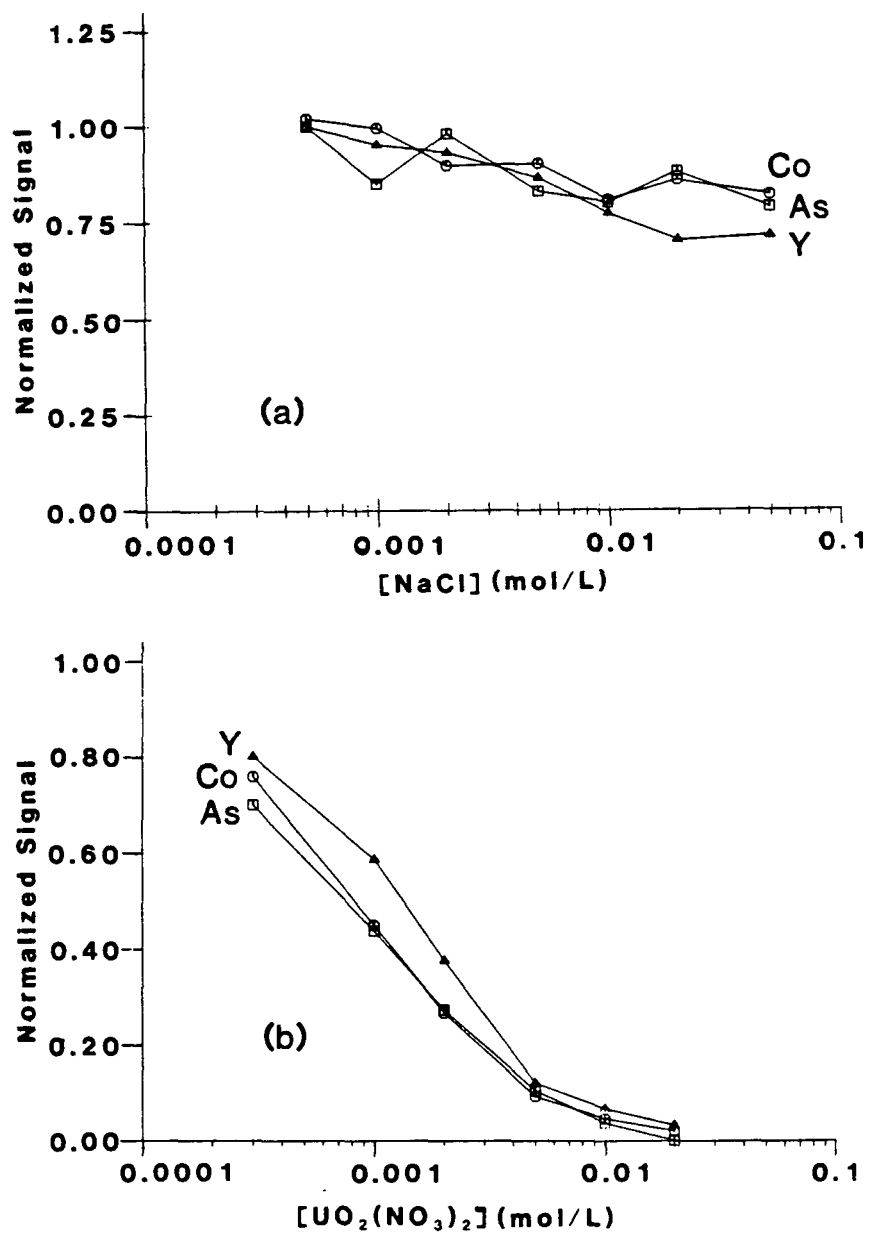Figure 4. Suppression of signal for Co (O), As (□) and Y (Δ) by
(a) NaCl and (b) $UO_2(NO_3)_2$ at $V_1 = +2.5$ V

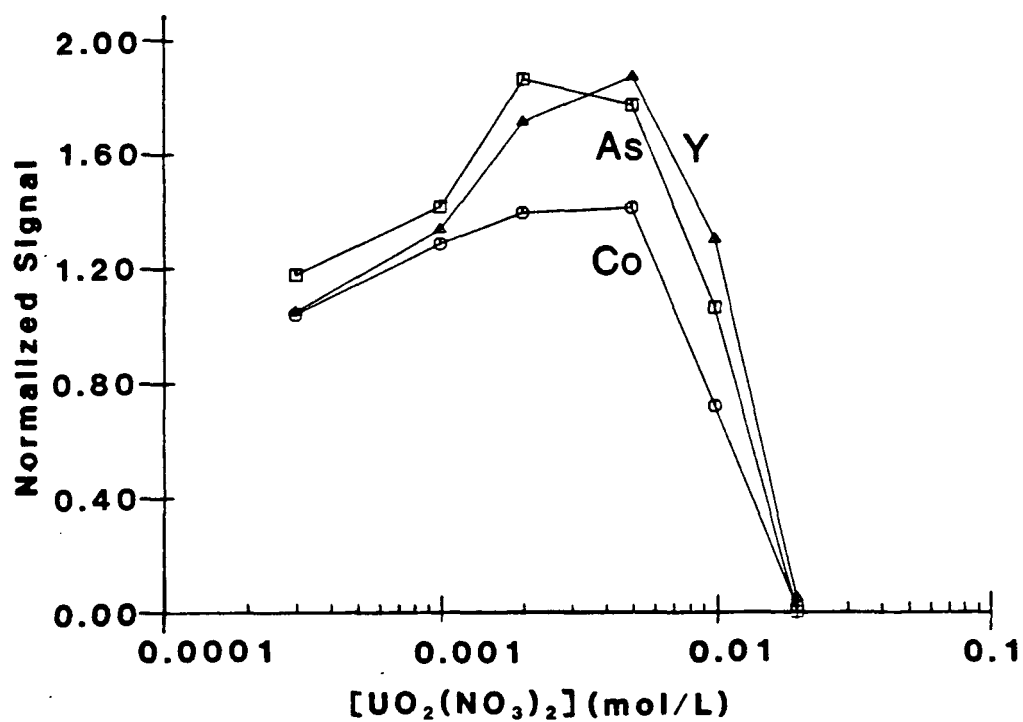Figure 5. Effect of $UO_2(NO_3)_2$ on Co (O), As (□) and Y (△) signal at V_1= +2.5 V. This figure differs from Figure 4b as described in the text

potentiometer) as a function of uranium matrix concentration indicated that the apparent cylinder bias changed as solutions having $UO_2(NO_3)_2$ concentrations exceeding 10^{-3} M were introduced into the ICP. The magnitude of this change was approximately 3 V. When the direction of this change was negative, the suppression behavior shown in Figure 4b was observed. When the apparent cylinder bias increased, signal enhancements like those in Figure 5 were observed.

The physical phenomena relating the ion optical properties described above to the observed interference behavior are as yet unclear. It would appear that these phenomena are in some way mass-dependent, since no such changes in apparent cylinder bias were observed for the lighter matrix elements under either of the ion optical conditions studied. Further investigations of the relationship between ion focusing and ion beam composition should clarify the relationship between ion optical parameters and interference measurements.

Effect of concomitant on ion kinetic energy

With skimmer a installed in the ICP-mass spectrometer, the kinetic energy of analyte ions was measured by applying a positive DC voltage to the mass filter so as to attenuate 90% of the analyte signal from solutions containing 1 mg L^{-1} of Co, As, and Y in the various matrices (10,11,13,14,28,29). These measurements were made at the plasma and ion optical conditions listed in Table 1. The results of these measurements are given in Table 3. All three analyte ions were cut off at essentially the same voltage, in agreement with the behavior reported by Gray and Williams (29). The ion energy was significantly positive, as usual for the load coil geometry employed (10,13,28,29). Under these

Table 3. Influence of Concomitant Salt Concentration on Ion Kinetic

Energy

[Salt] (mol L^{-1})	Cutoff Voltage for Co^+			
	$NaCl^a$	$NaCl^b$	$UO_2(NO_3)_2{}^a$	$UO_2(NO_3)_2{}^b$
0	13.9 ± 0.2^c	13.8	14.0	13.8
5×10^{-3}	14.0	14.1	15.2	15.1
10^{-2}	13.9	14.2	15.2	15.8^d
5×10^{-2}	13.8	14.1	–	–

$^aV_1 = -11.7$ V.

$^bV_1 = +2.5$ V.

^{c}Typical reproducibility for these measurements.

^{d}Orifice plugging by condensed uranium salts severe.

conditions, the kinetic energy of analyte ions was independent of the NaCl concentration in the sample matrix. In the presence of $UO_2(NO_3)_2$ at 5×10^{-3} M, the ion kinetic energies increased by approximately 1 eV. However, the kinetic energy did not change further with increasing $UO_2(NO_3)_2$ concentration. This observation indicated that the ion kinetic energies and hence, the focusing properties of the ion lens changed slightly in the presence of uranium, but any focusing error caused by such a change was consistent for each uranium interference measurement above 5×10^{-3} M.

It is interesting to note that, using skimmer a, the presence of U changed the kinetic energy for Co significantly (Table 3) but, with the same skimmer, the effect of U on Co signal (Figure 2) was about the same as that induced by other, lighter matrix elements that did not affect the ion energy. The ion kinetic energy did not depend on the voltage V_1 applied to the extraction cylinder, so it is considered likely that the ion lens did not influence the measured ion energies. However, significant plugging of the sampling orifice was noted for the entry labeled d in Table 3. Plugging caused the pressure in the expansion chamber to decrease from 600 mtorr to 500 mtorr, which corresponded to a reduction in orifice diameter by a factor of $((600-500)/600)^{1/2} \approx 16\%$. For the load coil geometry used in these experiments, reduction of the size of the orifice would be expected to intensify the secondary discharge and yield higher ion energies (30), as was observed. Thus, it is likely that plugging effects also influenced the interference of uranium on the analytes studied.

Conclusions

The present work indicates that the extent of matrix interferences in ICP-MS depends on a myriad of experimental parameters including ICP operating conditions, the identity of the matrix and the analyte, the geometry of the ICP-MS sampling interface, and the voltages applied to the ion optics of the instrument. From this result, it is obvious that interference phenomena involve complex interactions between these instrument parameters. More fundamental study will be required before an adequate mechanism for these interferences can be proposed. Based on the mass-dependent matrix interferences common to commercial ICP-mass spectrometers and the indication from the present work that such interferences may arise during the ion extraction and focusing steps, further investigations should focus on the spatial distribution of matrix and analyte species within the supersonic expansion, and the effect of these distributions upon ion transmission in the mass spectrometer. Such studies would have a large and immediate impact upon ICP-mass spectrometry. However, such experiments will not solve the current matrix interference problems. In the case of commercial ICP-MS instrumentation, some of the complexities associated with ICP-mass spectrometric analysis of concentrated salt solutions may be alleviated by careful consideration of the systematic variation of matrix interferences with analyte and matrix mass, such that the extent to which the matrix interferes with a given analyte may be anticipated. In addition, internal standardization can attenuate some interferences, provided that the internal standard is carefully selected (4).

Literature Cited

1. Houk, R.S.; Fassel, V.A.; Flesch, G.D.; Svec, H.J.; Gray, A.L.; Taylor, C.E. Anal. Chem. **1980**, *52*, 2283.

2. Date, A.R.; Gray, A.L. Analyst **1983**, *108*, 1033.

3. Olivares, J.A.; Houk, R.S. Anal. Chem. **1986**, *58*, 20.

4. Thompson, J.J.; Houk, R.S. Appl. Spectrosc. **1987**, *41*, 801.

5. Beauchemin, D.; McLaren, J.W.; Berman, S.S. Spectrochim. Acta, Part B **1987**, *42B*, 467.

6. Gregoire, D.C. Appl. Spectrosc. **1987**, *41*, 897.

7. Gregoire, D.C. Spectrochim. Acta, Part B **1987**, *42B*, 895.

8. Tan, S.H.; Horlick, G. J. Anal. Atomic Spectrom. **1987**, *2*, 745.

9. Gillson, G.R.; Douglas, D.J.; Fulford, J.E.; Halligan, K.W.; Tanner, S.D. Anal. Chem. **1988**, *60*, 1472.

10. Douglas, D.J.; French, J.B. Spectrochim. Acta, Part B **1986**, *41B*. 197.

11. Fulford, J.E.; Douglas, D.J. Appl. Spectrosc. **1986**, *40*, 971.

12. Houk, R.S.; Schoer, J.K.; Crain, J.S. J. Anal. Atomic Spectrom. **1987**, *2*, 283.

13. Gray, A.L.; Houk, R.S.; Williams, J.G. J. Anal. Atomic Spectrom. **1987**, *2*, 2.

14. Gray, A.L. J. Anal. Atomic Spectrom. **1986**, *1*, 247.

15. Kawaguchi, H.; Tanaka, T.; Nakamura, T.; Morishita, M.; Mizuike, A. Anal. Sci. **1987**, *3*, 305.

16. Olivares, J.A.; Houk, R.S. Anal. Chem. **1985**, *57*, 2674.

17. Scott, R.H.; Fassel, V.A.; Kniseley R.N.; Nixon, D.E. Anal. Chem. **1974**, *46*, 75.

18. Bear, B.R.; Fassel, V.A. Spectrochim. Acta, Part B **1986**, 41B, 1089.

19. Olson, K.W.; Haas, W.J. Jr.; Fassel, V.A. Anal. Chem. **1977**, 49, 632.

20. Koirtyohann, S.R.; Jones, J.S.; Yates, D.A. Anal. Chem. **1980**, 52, 1965.

21. Douglas, D.J.; French, J.B. J. Anal. Atomic Spectrom. **1988**, 3, 743.

22. Douglas, D.J.; Kerr, L.A. J. Anal. Atomic Spectrom. **1988**, 3, 749.

23. Horlick, G.; Tan, S.H.; Vaughan, M.A.; Rose, C.A. Spectrochim. Acta, Part B **1985**, 40B, 1555.

24. Vaughan, M.A.; Horlick, G. J. Anal. Atomic Spectrom. **1987**, 2, 765.

25. Houk, R.S.; Svec, H.J.; Fassel, V.A. Appl. Spectrosc. **1981**, 35, 380.

26. Kalnicky, D.J.; Kniseley, R.N.; Fassel, V.A. Appl. Spectrosc. **1977**, 31, 137.

27. de Galan, L.; Smith, R.; Winefordner, J.D. Spectrochim. Acta, Part B **1968**, 23B, 521.

28. Olivares, J.A.; Houk, R.S. Appl. Spectrosc. **1985**, 39, 1070.

29. Gray, A.L.; Williams, J.G. J. Anal. Atomic Spectrom. **1987**, 2, 599.

30. Houk, R.S. Ames Laboratory-USDOE, unpublished data.

59

SECTION III.

MASS SPECTROMETRIC MEASUREMENT OF IONIZATION TEMPERATURE IN AN

INDUCTIVELY COUPLED PLASMA

Introduction

Since the construction of the first inductively coupled plasma-mass

spectrometer in the late 1970s (1), various investigators have tried to

use the MS as a tool for the measurement of ionization temperature

(hereafter called T_{ion}) in the ICP. The reasoning behind this

experiment is simple. Because the mass spectrometer samples ions

directly from the plasma, it can be used to measure elemental degrees of

ionization. These quantities could be used in turn to calculate T_{ion}

using the Saha equation (2,3), given a value of electron density

characteristic of the point at which the ICP is sampled. Because of the

radially resolved nature of ICP-MS sampling, this measurement technique

would obviate the need for Abel inversion (4), which is used in optical

emission experiments to construct radial emission profiles from line-of-

sight intensity measurements. Such Abel techniques also induce

substantial imprecision in the measured emission profiles. Thus, mass

spectrometric methods would be expected to produce more reliable T_{ion}

values, provided that the relative ion abundances measured by the mass

spectrometer reflect the relative population of ions in the plasma.

The earliest studies in this area were performed on an instrument

which sampled ions from an aerodynamic and electrostatic boundary layer

upstream of a small (< 50 μm diameter) sampling orifice in a flat

molybdenum disk (2,5). The temperatures measured with this instrument, although in a range considered "typical" of the ICP (~7500 K at n_e = 10^{15} cm^{-3}) (6), were of questionable diagnostic value owing to perturbations in the composition of the ionic sample. These perturbations arose from two sources, the first being enhanced recombination and chemical reactions in the boundary layer, as indicated by the high levels of polyatomic analyte species (e.g., MO^+ and MOH^+) found in the mass spectra. The second source of perturbation was indicated by high levels of doubly charged ions (e.g., Ar^{2+}) in the mass spectra, which may have been due to the presence of a strong secondary discharge within the vacuum chamber itself. Such perturbations of the ion sample are undesirable for characterization of plasma properties such as temperature.

Use of a continuum-flow interface attenuated the problem of boundary layer reactions indicated in the mass spectra (7,8). However, the problems commensurate with the presence of a secondary discharge seem to persist, although the discharges in current ICP-MS instruments are characteristic of an electrical interaction between the plasma and the grounded sampling cone (9). The problems created by such discharges are evident in recent reports showing that T_{ion}, as measured by mass spectrometry, changes little with variation in aerosol gas flow rate (3,10), but increases sharply with increasing sampler-load coil separation (3). These observations are in direct contradiction of trends previously reported by ICP optical emission measurements of T_{ion} (11), and might be more consistent with a juxtaposition of the secondary discharge and the ICP (3). Douglas and French (9) have shown that this

discharge can be effectively eliminated by use of a center-tapped load coil. Furthermore, the strength of this discharge can be attenuated by empirical "tuning" of the load coil (9,12,13), i.e., choosing a load coil and grounding position on the load coil which minimizes the intensity of this discharge, as determined by measurement of plasma potential and ion kinetic energy (13,14). Thus, the combination of continuum-flow sampling and careful load coil "tuning" should permit reliable mass spectrometric measurement of T_{ion}.

The present work describes the optical measurement of electron density just upstream of the sampling interface, and the subsequent calculation of T_{ion} using the Saha equation and degrees of ionization measured by mass spectrometry. The variation of electron density and T_{ion} with ICP operating parameters is reported, and the effect of a weak but persistent secondary discharge on these measurements is described, as are element-to-element differences in observed ionization temperatures. These data are compared with those from a commercial ICP-MS instrument with a center-tapped load coil.

Experimental

Electron density measurement

In this study, electron density was measured by determining the extent of Stark broadening for the H I emission line at 486.13 nm. An image of the plasma-mass spectrometer interface was focused on the entrance slit of a 0.5 m Ebert monochromator using a pyrex lens (f/2, magnification 1.6). The optics and monochromator have been described previously, as has the arrangement of these components with respect to the interface (15). The effective observation zone of this apparatus

was an area 16 μm wide by 1.25 mm long approximately 0.8 mm upstream of the mass spectrometer sampling orifice, centered on the orifice. The axial channel of the ICP was centered on the sampling orifice as well. The monochromator was scanned from 483 nm to 490 nm, and the resulting spectrum was stored in a 4096-channel multichannel analyzer after conversion of the photocurrent to TTL pulses using a current-to-frequency converter. These components have also been described (15). A distilled, doubly deionized water blank was introduced into the ICP during these measurements to eliminate the possibility of spectral interferences from the analytes used in this study. In general, the photocurrent produced by the PMT at the peak of the H I emission was ca. 400 nA on a background of ca. 30 nA. These values varied by ± 20% over the range of plasma operating conditions used.

The full width at half-maximum (FWHM) of the H I emission was measured by calibrating the horizontal scale of the multichannel analyzer in wavelength units using the channels corresponding to the maximum intensity of the Ar I emission lines at 487.63 nm and 488.795 nm. These data were used to calculate electron density using the method described by Kalnicky et al. (16). A FORTRAN computer program called NECALC was used to perform these calculations (see the Appendix). Lateral intensity profiles from the ICP alone for H I emission were measured. Abel inversion of those profiles indicated that the FWHM of the H I emission line from the center of the ICP was not significantly different from that of the lateral intensity measurements. Thus, in these experiments, electron densities calculated from lateral emission measurements would not differ substantially from calculations using

radially-resolved intensity measurements. However, self-absorption of the H I emission was clearly evident in the lateral intensity measurements, thereby introducing error into the determination of the maximum emission intensity and consequently introducing error into the FWHM measurement. Electron densities measured in these experiments fell between 1.5×10^{15} cm^{-3} and 4.0×10^{14} cm^{-3}. Repetitive measurements of n_e had a relative standard deviation (RSD) of $\pm$ 6%.

Ionization temperature measurement

The ICP-MS instrument used in this study has been described previously (15,17). A solution containing 1 mg L^{-1} Sb and In (m/z 121, 123 and m/z 113 and 115, respectively) and 2 mg L^{-1} As and Ga (m/z 75 and m/z 69 and 71, respectively) was introduced into the ICP. These elements were chosen because the elements in each pair had similar masses, but had substantially different ionization energies. The mass spectra of these elements were acquired at the ICP-MS operating conditions described in Table 1. These conditions corresponded to points near the maximum of the parameter behavior plot (18,19) for this particular ICP-MS instrument. Introduction of distilled, deionized water during the course of these measurements showed no indication of isobaric interferences on any of the analytes used.

A ratio of the sum of net isotopic peak areas for each elemental pair (Sb/In and As/Ga) was calculated and was corrected for differences in the molarity of each element in solution. The Sb/In ratio was measured with a typical RSD of $\pm$ 0.3%, and As/Ga ratios were typically measured with an RSD of $\pm$ 1.2%. Because the elements in each pair were

Table 1. Instrumental Components

Component	Operating Conditions

ICP torch and generator	argon flow rates $(L\ min^{-1})$:
	    outer: 15.6
	   aerosol: 0.95 ± 0.2
	  auxiliary: only used during
	         ICP startup
	forward power: 1.4 ± 0.1 kW
	reflected power: <5 W
	load coil grounded at turn closest
	to sampler

nebulizer (15)	solution uptake rate: 2.5 mL min^{-1} desolvation temperature: 140°C
ion extraction interface	sampling position: 12 ± 2 mm above top of coil, axial channel centered on sampling orifice operating pressure: ~ 1.1 torr
ion optics	applied voltages: first cylindrical lens: -41, photon baffle: -6.7, second cylindrical lens: +19.5, third " " : -89.6, fourth " " : -63.2, differential pumping orifice: -30, ELFS lens: -60
mass analyzer	rod bias (V): +1 FWHM resolution at m/z 71: 95
detector assembly (15)	quadrupole exit lens: -480 V ion deflecting plate: +900 V detector housing aperture: -1250 V
detector	operating voltage: -3 kV approximate gain = 10^{7}
current-to-frequency conversion (15)	sensitivity: 10^{-12} A Hz^{-1}

multichannel analyzer	dwell time/channel: 200 μs (MS)
	                20 ms (AES)
	channels: 4096
	sweeps: 50-100 (MS)
	       1 (AES)

close in m/z and the resolution of the mass filter was purposely set low, the transmission of their ions through the mass spectrometer should not have differed greatly, such that these ratios accurately reflected the relative degree of ionization for the elements in each pair. Ionization temperature was then calculated from these data using a FORTRAN computer program called TCALC (see the Appendix). To perform this calculation, partition functions for the reference element (i.e., In or Ga) and the thermometric element (Sb or As) were calculated at an arbitrary starting temperature (20,21). At the measured n_e, the degree of ionization (α) (2) for the reference element was calculated using the Saha equation, and α for the thermometric element was found using the relative degree of ionization for the thermometric pair. Solving the Saha equation for α of the thermometric element yielded a new T_{ion}. Using the new T_{ion}, this procedure was iterated until T_{ion} converged to within 0.1% of its previous value. Propagation of experimental uncertainties showed that these temperatures had RSDs of ~ 0.5%.

<div align="center">Results and Discussion</div>

Electron density measurements

Figure 1 illustrates the variation in electron density with axial position for the Stark broadening measurements described above. The figure shows that the electron density in the plasma just upstream of the sampling orifice decreases with increasing sampler-load coil separation, increasing aerosol gas flow rate, and decreasing ICP forward power. The magnitude of these electron densities and the trends shown agree closely with those observed in ICPs used for optical emission alone (11,22,23). However, it should be noted that, because of a lack
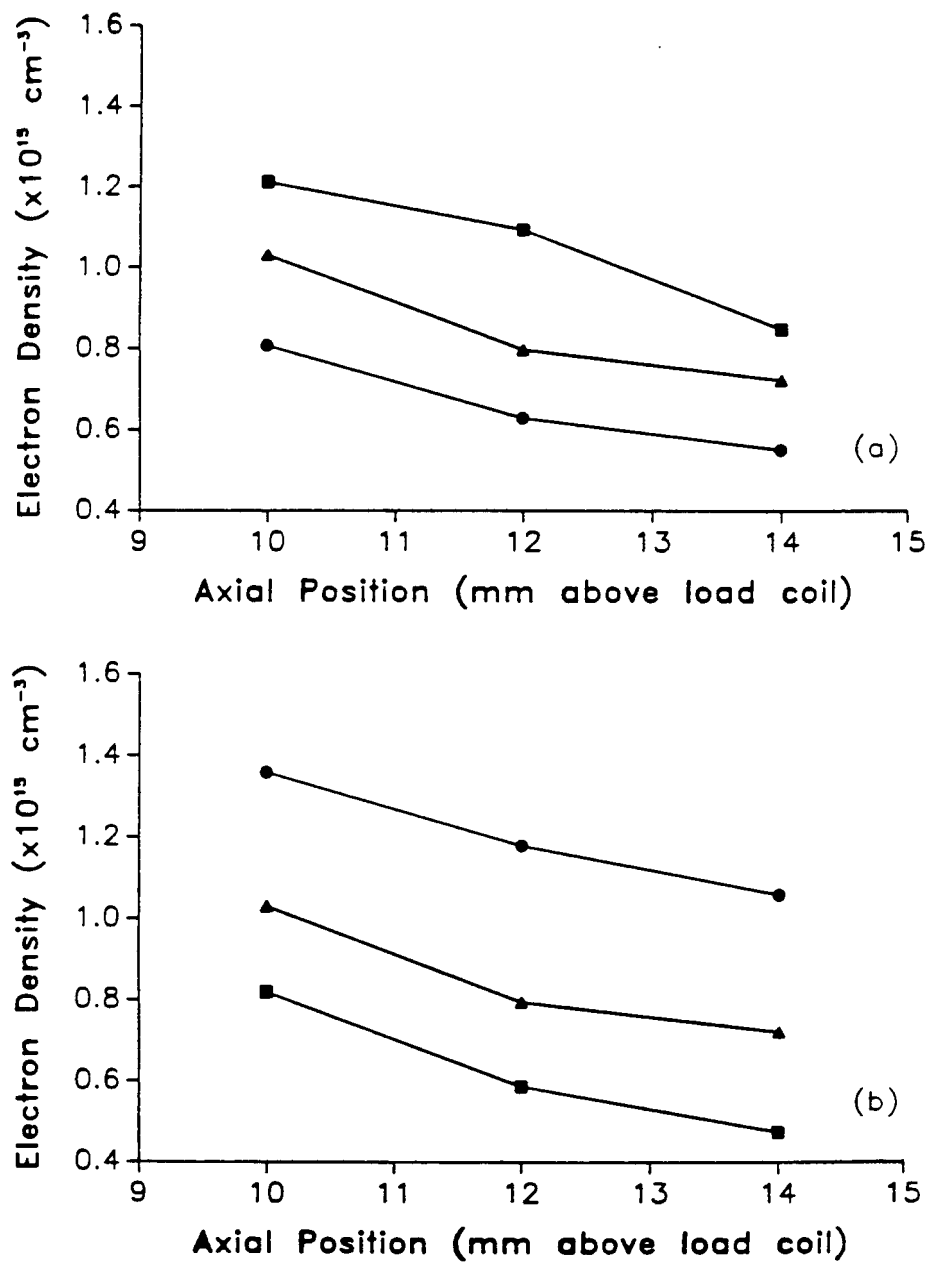
Figure 1. Variation of electron density upstream of sampler with sampler-load coil separation at: (a) 0.95 L min^{-1} aerosol gas flow rate and 1.3 kW (●), 1.4 kW (▲), and 1.5 kW (■); (b) 1.4 kW forward power and 0.75 L min^{-1} (●), 0.95 L min^{-1} (▲), and 1.15 L min^{-1} (■)

of strong OH band emission in the wavelength region between ca. 305 nm

and ca. 320 nm, it was not possible to calculate an ICP gas temperature

(T_{gas}) based on the relative strengths of lines within the OH band

structure (24). The effect of this problem is as follows: The FWHM of

the H I emission will be the result of a number of spectral broadening

effects, including Stark and Doppler broadening. To accurately

calculate electron density from these data, it is necessary to correct

the measured linewidths for other broadening effects. The correction

for pressure and instrumental broadening will remain essentially

constant throughout the course of an given experiment, however, the

Stark and Doppler broadening components will vary with plasma

conditions. If T_{gas} is not known, then accurate correction for Doppler

broadening is not possible. Therefore, in the present work, n_e was

calculated at an arbitrary T_{gas} of 5000 K. This fact unquestionably

induces some calculational error into the electron densities. However,

over the range of electron densities considered reasonable for the ICP

used in this work (3×10^{14} cm^{-3} to 3×10^{15} cm^{-3}), the variation in the

reduced Stark half-width parameter used in these calculations (16) is

only 4 to 6% over the range of gas temperatures considered reasonable

(5000 K to 10 000 K). Therefore, calculational errors, although

present, should not be particularly severe for the ICP conditions used

in this work, implying that at least the trends shown are representative

of the behavior in electron density upstream of the sampling orifice.

In a study such as this, it is important to determine the sampling

accuracy of the measurement technique, i.e., is the mass spectrum

affected by artifacts of the extraction process? From the properties of

isentropic expansions, Douglas and French (25) have concluded that an ICP-mass spectrometer draws a representative sample of ions from the ICP. However, this conclusion is not easily confirmed by non-spectroscopic means. Therefore, an experiment was performed in which the electron density in the ICP alone (i.e., when the ICP was not being sampled for mass spectrometry) was compared to that upstream of the sampling interface of the mass spectrometer for identical ICP conditions and several optical observation heights. This comparison is shown in Figure 2. Within the experimental uncertainty in electron density discussed above, it can be seen that electron density in the ICP is similar to that at the sampling interface. Thus, the total charge density in the plasma gas just upstream of the sampler is similar to that in an unperturbed plasma. This observation conditionally confirms the validity of the present work, as well as previous mass spectrometric measurements of T_{ion}.

For the purpose of further comparison, the electron density in an aerodynamic boundary layer upstream of the sampling orifice was measured and compared to that in the ICP alone. The result of this experiment is also shown in Figure 2. To construct such a boundary layer, the mass spectrometer was shut down and the vacuum chamber was filled with dry, room temperature argon such that a thick, visible boundary layer formed around the tip of the sampling cone. This layer was not due to an outward flow of argon from the vacuum chamber, since the vent to the chamber was kept open after filling to equalize the pressure between the interface and the plasma. Thus, the electron density measurements were representative of the boundary layer being formed by the hot plasma
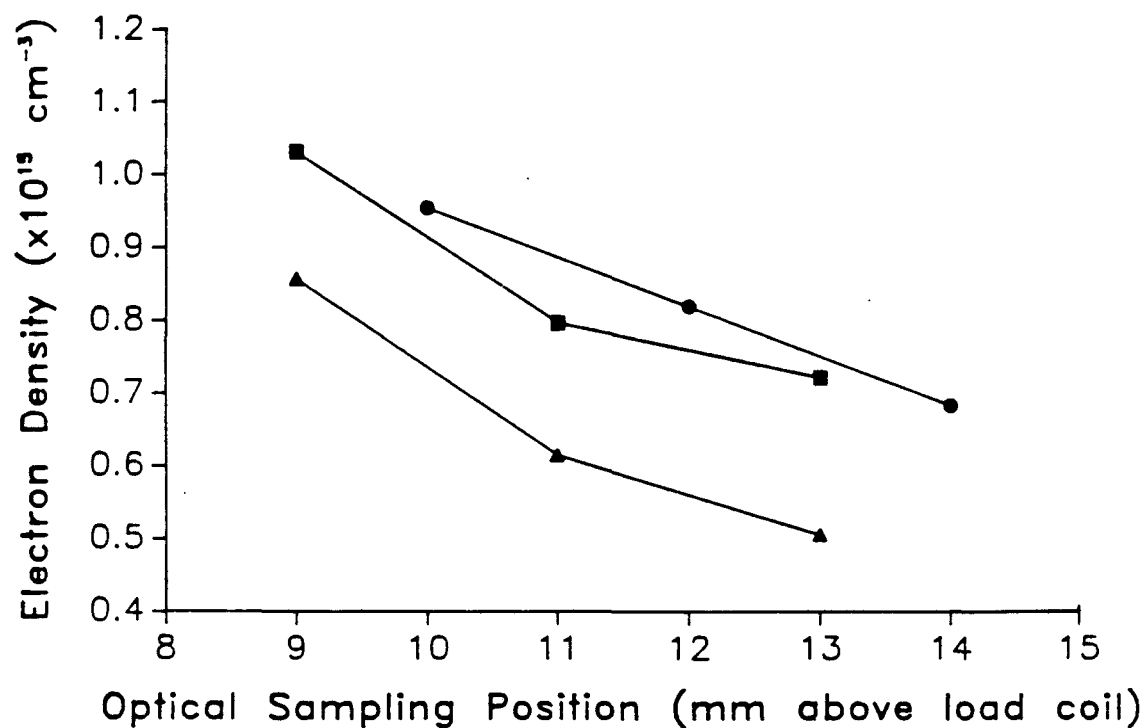
Figure 2. Variation of electron density with optical sampling
position at 1.4 kW forward power and 0.95 L min^{-1} aerosol
gas flow rate under several ICP sampling situations.
Electron density at mass spectrometer interface during
sampling (■), electron density in ICP alone (●), and
electron density in boundary layer (▲)

gases. The electron density measured in this layer was somewhat lower than that in the plasma alone, which is consistent with the fact that recombination is known to be facile in boundary layers. However, the boundary layer thickness at the end of the cone was such that the optical spectrometer still observed part of the ICP, as well as part of the boundary layer. Therefore, the electron density shown is at best an average of that in the ICP and the boundary layer.

Ionization temperature measurements

The variation of ionization temperature with ICP forward power at constant aerosol gas flow rate and several sampler-load coil separations is shown in Figure 3. Figure 3a shows the variation in Sb ionization temperature, while Figure 3b shows that for As. These data indicate that T_{ion} for both elements increased almost linearly with increased forward power. These increases are significantly greater than the experimental uncertainty associated with these T_{ion} measurements. The magnitude of the measured T_{ion}s and their variation with forward power are consistent with previous T_{ion} measurements by optical emission (23) and mass spectrometry (2,3). These data also show that the variation of T_{ion} with sampler-load coil separation is weak for both elements, and in the case of Sb, is less than the experimental uncertainty. This observation agrees with those made in other optical emission measurements of T_{ion} (11), but contradict observations reported in the mass spectrometric measurements of T_{ion} referenced earlier (3). Table 2 shows the change in the maximum kinetic energy of $^{69}Ga^+$ with variation in forward power and sampler-load coil separation. The changes in ion kinetic energy indicate that the mild secondary discharge present in
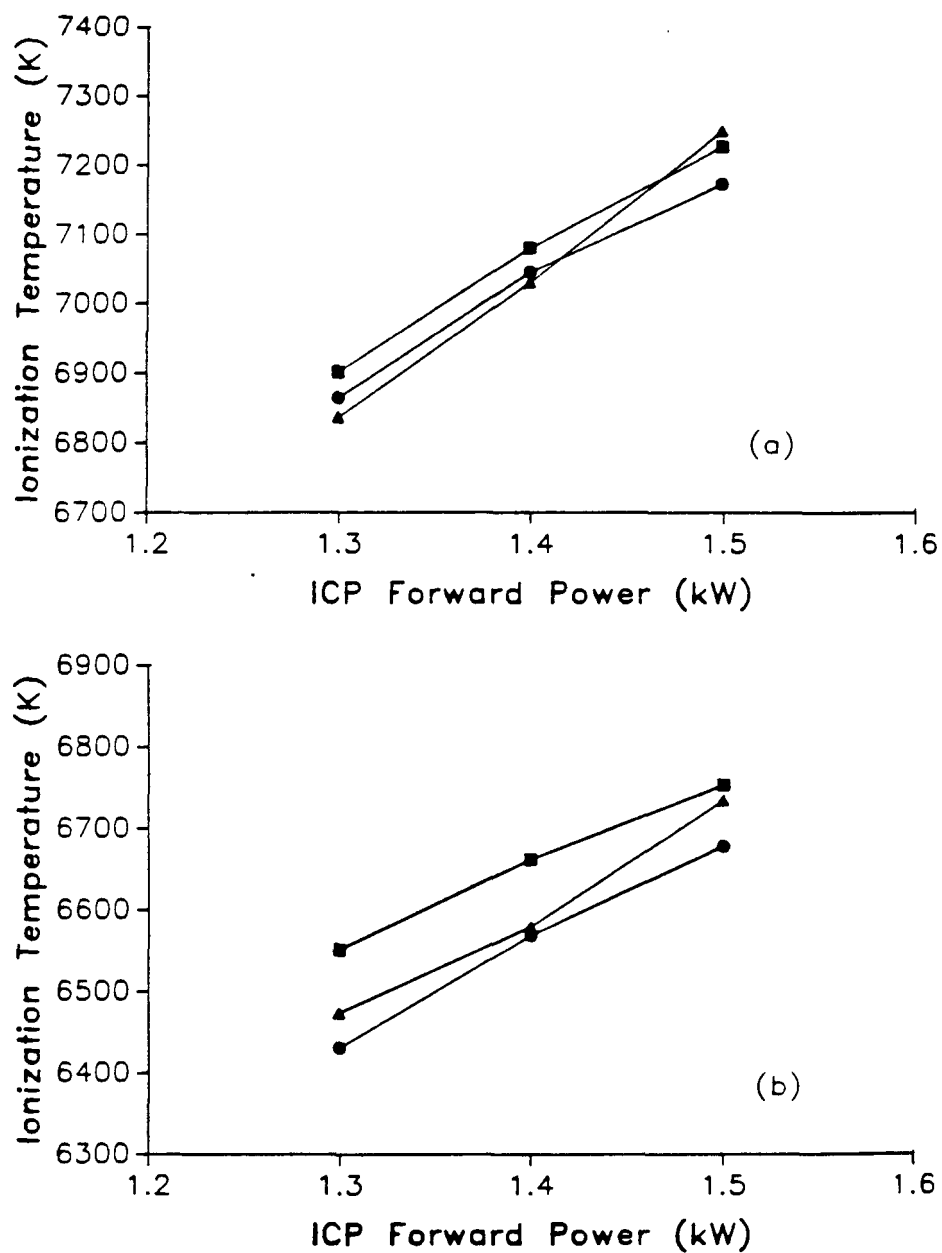
Figure 3. Variation of ionization temperature with ICP forward
power at 0.95 L min^{-1} aerosol gas flow rate and several
sampler-load coil separations for: (a) Sb at 10 mm (■),
12 mm (▲), and 14 mm (●); (b) As at 10 mm (■), 12 mm
(▲), and 14 mm (●)

Table 2. Influence of ICP-MS Operating Parameters on Kinetic Energy of
$^{69}Ga^+$ at 0.95 L min^{-1} Aerosol Gas Flow Rate

Power (kW)	Ion Kinetic Energies (eV) at Indicated Sampler-Load Coil Separation[a]		
	10 mm	12	14
1.3	11.4 ± 0.2[b]	10.5	10.1
1.4	10.1	9.0	8.1
1.5	9.3	8.4	7.9

[a]The entries in this table represent the energy at which 100% of the $^{69}Ga^+$ signal was attenuated (14,15).

[b]Typical range of these measurements.

this particular ICP-MS instrument grew weaker as forward power and sampler-load coil separation were increased. Thus, the trends described above for ionization temperature must be characteristic of the ICP itself, even though the temperature values may be influenced by the presence of the secondary discharge.

The dependence of As ionization temperature on position as shown in Figure 3b, although weak, may indicate that the ionization kinetics of As are different than those of Sb, thus inducing a stronger temperature-position dependence for As. Another indication of these kinetic differences can be seen in the significant difference between the numerical value of ionization temperature for Sb and As. Such differences are also evident in Figure 4. It has been proposed that interelement differences in ionization temperature would arise in optical emission measurements from element-to-element variation in the kinetics of certain de-excitation processes (26). From the data presented here, it would also appear that similar considerations apply to the kinetics of the ionization process as well, since the kinetics of ionization and recombination will determine the ionization temperature measured by mass spectrometry.

The variation of ionization temperature with aerosol gas flow rate at constant sampler-load coil separation and several forward powers is shown in Figure 4. Sb ionization temperature decreased with increasing aerosol gas flow rate (Figure 4a). This trend has been observed in previous T_{ion} measurements by optical emission (11). However, previous investigators reported little variation in mass spectrometric measurement of T_{ion} with aerosol gas flow rate (3,10). The reason for
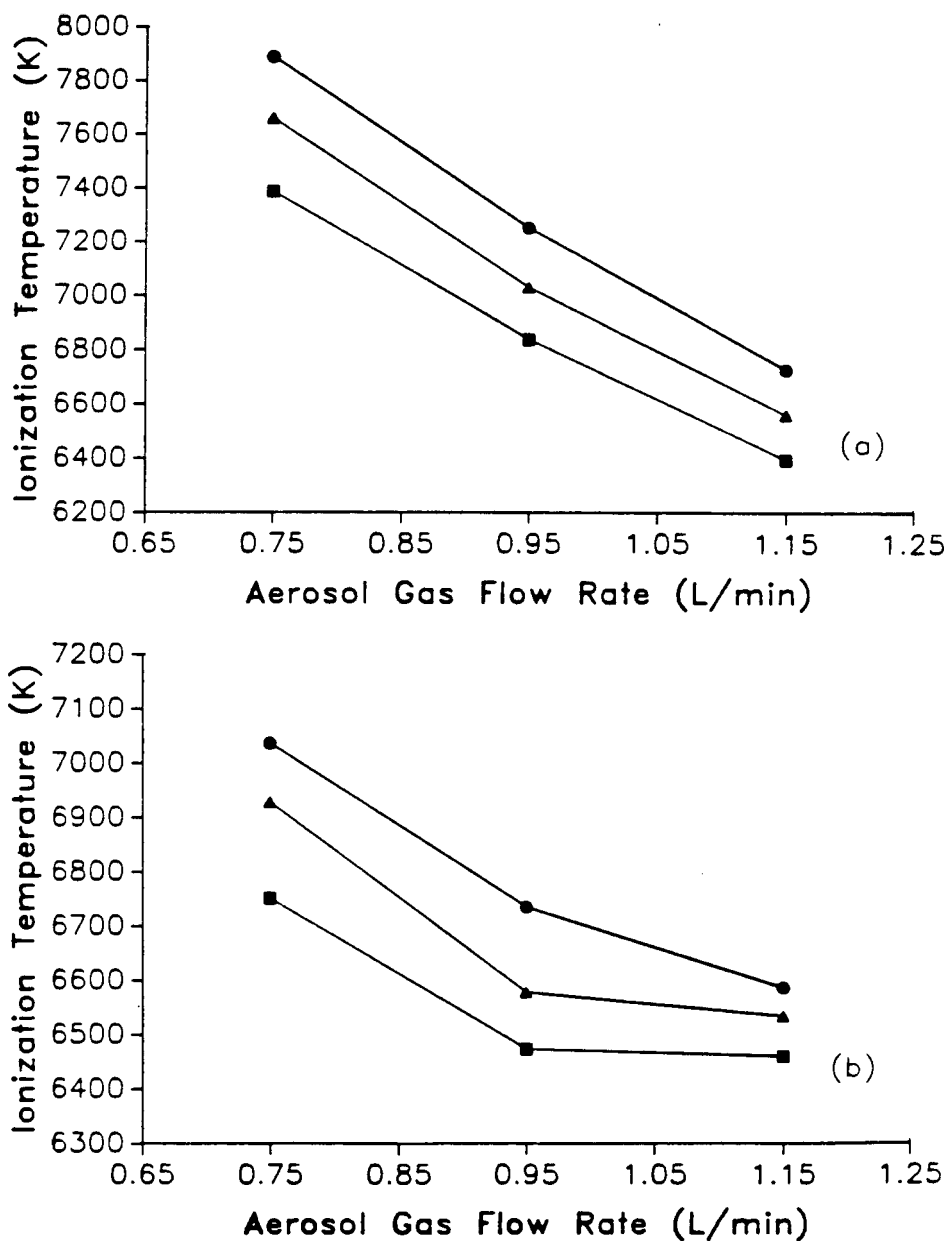
Figure 4. Variation of ionization temperature with aerosol gas flow
rate at 12 mm sampler-load coil separation and several
ICP forward powers for: (a) Sb at 1.3 kW (■), 1.4 kW
(▲), and 1.5 kW (●); (b) As at 1.3 kW (■), 1.4 kW
(▲), and 1.5 kW (●)

such reports can be deduced from data shown in Figure 4b and Table 3. Figure 4b clearly shows that the As ionization temperature remained essentially constant as aerosol gas flow rate was increased above 0.95 L min^{-1} at powers less than 1.4 kW. Based on the ion kinetic energies given in Table 3, these conditions also intensified the secondary discharge at the sampling interface, as indicated by the increase in kinetic energies with aerosol gas flow rate. Thus, the intensification of this discharge appears to exert an influence upon the As ionization temperature.

Apparently, for reasons that are not clear, this discharge does not affect the ionization temperature of Sb. However, Figure 5 illustrates one possible explanation. These data indicate that the degree of ionization for Sb (i.e., the fraction of Sb ionized by the plasma), which is more extensive than that of As, decreased smoothly with increasing aerosol gas flow rate, while that of As increased sharply at 1.15 L min^{-1}. The trend for Sb is consistent with that observed in optical emission measurements of degrees of ionization for Cd (23). From this observation, Sb probably traverses the secondary discharge without significant perturbation to the ion/atom ratio, even under conditions which increase the severity of this discharge, while As is not able to do so. This phenomenon may be due to the interelement differences in ionization kinetics described earlier. Thus, temperature calculations for Sb would be valid using the electron density measured upstream of the sampling orifice, while the same calculations for As would require correction for the influence of the secondary discharge upon As ionization.

Table 3. Influence of ICP-MS Operating Parameters on Kinetic Energy of
$^{69}Ga^+$ at 12 mm Load Coil-Sampler Separation

	Ion Kinetic Energies (eV) at Indicated Aerosol Gas Flow Rates[a]		
Power (kW)	0.75 L min^{-1}	0.95	1.15
1.3	6.2	10.5	>15
1.4	5.9	9.0	>15
1.5	$-$ [b]	8.4	14.9

[a]The entries in this table were measured in the same manner as those in Table 2.

[b]Signal from $^{69}Ga^+$ was insufficient to measure an energy.
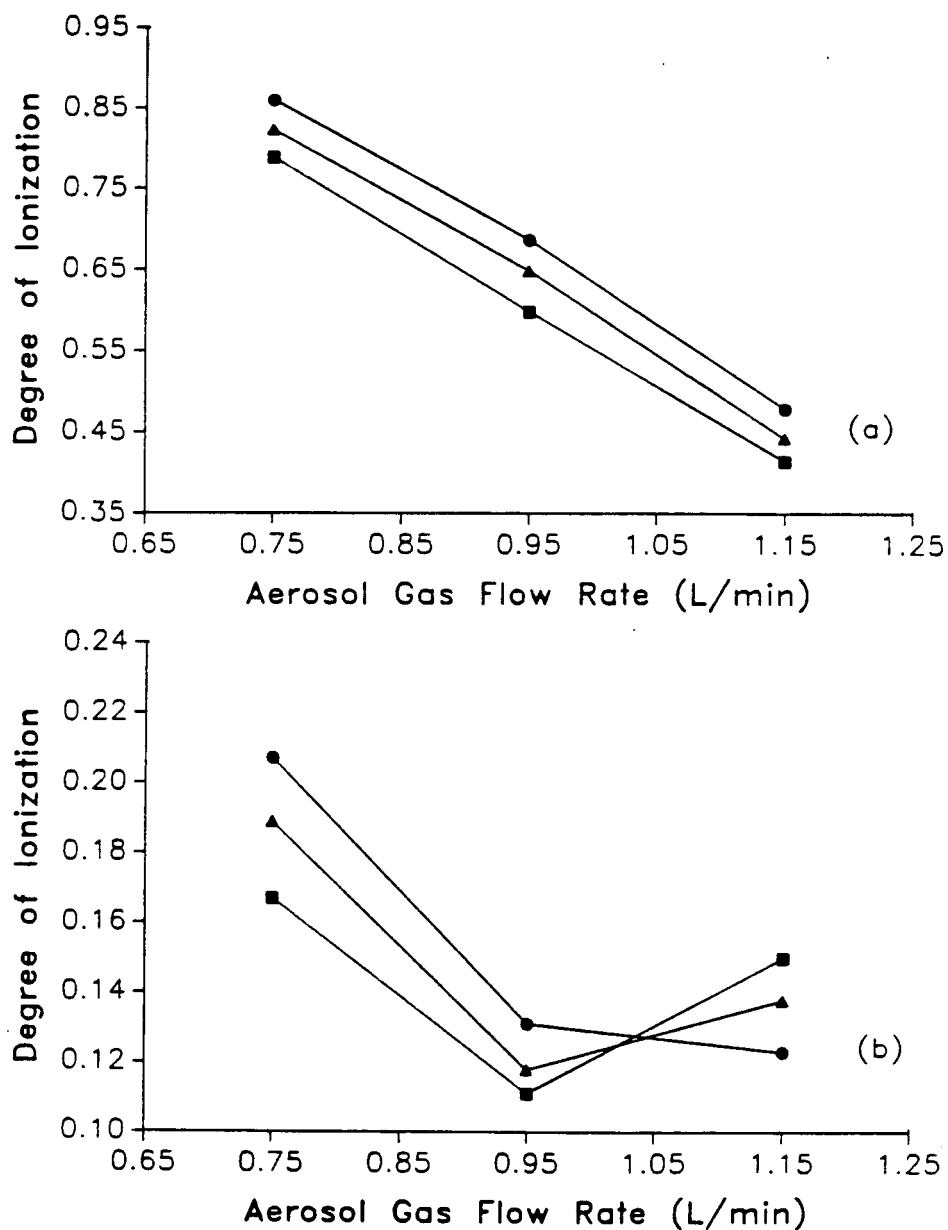
Figure 5. Variation in degree of ionization with aerosol gas flow
          rate at 12 mm sampler-load coil separation and several
          ICP forward powers for: (a) Sb at 1.3 kW (■), 1.4 kW
          (▲), and 1.5 kW (●); (b) As at 1.3 kW (■), 1.4 kW
          (▲), and 1.5 kW (●)

For the purpose of comparison, a similar experiment was performed
on a Perkin-Elmer Sciex ELAN model 250 ICP-mass spectrometer. The Ames
ELAN has been described previously (27), and the operating conditions
used in these measurements are given in Table 4. These conditions
corresponded to points in and around the the maximum of the parameter
behavior plot for this instrument, but were different than those given
in Table 1 for the "home-made" ICP-MS instrument owing to fundamental
design differences between the two. The degree of ionization
measurements were made in a fashion similar to those already described,
and ionization temperatures were calculated using the electron densities
given in Table 5. The results of these calculations can be seen in
Figure 6. With this device, ionization temperature for both elements
declined substantially at high aerosol gas flow rate, especially at low
forward power. The ELAN sampling interface has been designed in a way
which nearly eliminates the presence of a secondary discharge, primarily
through the use of a center-tapped load coil (9,28). Therefore, the
trends observed on the ELAN should not be influenced by the presence of
a secondary discharge, and they should be characteristic of processes
occurring in the ICP itself. Direct comparison of Figures 4 and 6 show
that, although the trend of decreasing temperature with increasing
aerosol gas flow rate is roughly consistent between the two instruments,
the temperature values measured on the ELAN are significantly lower than
those measured on the "home-made" instrument. Furthermore, the
interelement differences in ionization temperature described earlier are
not seen from the ELAN measurements. However, such comparisons may not
be entirely valid in the present work, since the forward power and

Table 4. Perkin-Elmer Sciex ELAN Operating Conditions

ICP torch	Ames Laboratory design (29); outer tube extended 30 mm beyond inner tubes.
forward power	0.95 kW ± 0.1 kW
argon flow rates (L min^{-1})	outer: 12.0 aerosol: 1.4 ± 0.2 auxiliary: 0.4
sampling position	15 mm above load coil, axial channel centered on sampling orifice
sampler	nickel, 1.2 mm orifice
skimmer	nickel, 0.90 mm orifice

ion optics
    Bessel box barrel
    Bessel box plate lenses
    Einzel lenses 1 and 3
    Einzel lens 2
    Bessel box photon stop
	upgraded version
	+5.4 V
	-10.9 V
	-19.8 V
	-130 V
	-4.9 V

operating pressures	interface: ~ 1 torr main chamber: 4×10^{-5} torr
data acquisition	mode: multielement measurement time: 0.5 s dwell time: 25 ms measurements/peak: 20

Table 5. Electron Densities Used in Calculation of Ionization

Temperature for an ICP-MS Instrument with a Center-Tapped Load

Coil

Power (kW)	Electron Density ($\times 10^{14}$ cm^{-3}) at Indicated Aerosol Gas Flow Rates[a]		
	1.20 L min^{-1}	1.40	1.60
0.85	7.0	5.7	4.8
0.95	8.2	7.0	5.9
1.05	9.5	8.1	7.0

[a]The entries in this table were estimated from data in references 11 and 22.
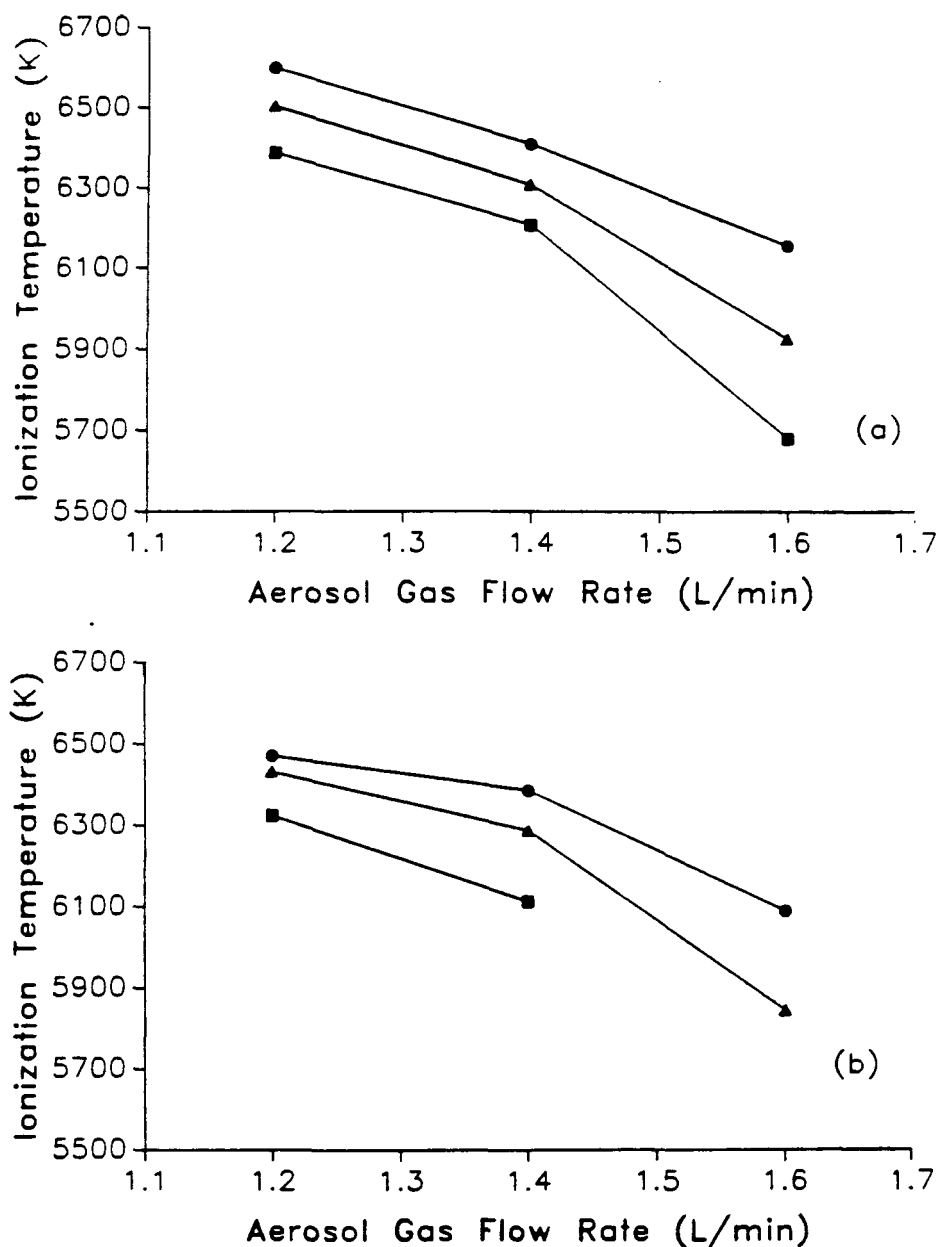
Figure 6.   Variation of ionization temperature with aerosol gas flow
            rate at 15 mm sampler-load coil separation and several
            ICP forward powers for an ICP-MS instrument with a
            center-tapped load coil. (a) Sb at 0.85 kW (■), 0.95 kW
            (▲), and 1.05 kW (●); (b) As at 0.85 kW (■), 0.95 kW
            (▲), and 1.05 kW (●)

aerosol gas flow rate necessary to obtain optimum ion signal differed substantially for the two instruments, and the electron densities used to calculate ionization temperature from the ELAN degrees of ionization were arbitrary.

Conclusions

This work indicates that mass spectrometry can be used reliably as a means of measuring ionization temperature for various elements in an inductively coupled plasma, even if a mild secondary discharge persists between the plasma and the sampling interface of the mass spectrometer. However, it appears that the choice of a thermometric element cannot be made arbitrarily, since the present work indicates that element-to-element variations exist in both the measured temperature value and the variation of temperature with plasma conditions. The cause of these element-to-element variations are as yet unclear. This phenomenon not only affects temperature measurements, but also affects the extent to which different elements are influenced by the presence of a secondary discharge (see Figure 5). Spectroscopic and electrical studies of the ICP-MS sampling interface may indicate the fundamental cause of this effect. However, it is interesting to note that the measured ionization temperatures of As and Sb varied uniformly with changes of plasma operating conditions in an ICP-mass spectrometer with a center-tapped load coil. This result suggests that "compromise" ionization conditions may be more difficult to attain for an instrument with a persistent secondary discharge, since the analytes in a sample may behave differently as the secondary discharge is attenuated or intensified.

83

Literature Cited

1. Houk, R.S.; Fassel, V.A.; Flesch, G.D.; Svec, H.J.; Gray, A.L; Taylor, C.E. Anal. Chem. 1980, 52, 2283.

2. Houk, R.S.; Svec, H.J.; Fassel, V.A. Appl. Spectrosc. 1981, 35, 380.

3. Wilson, D.A.; Vickers, G.H.; Hieftje, G.H. Appl. Spectrosc. 1987, 41, 875.

4. Cremers, C.J.; Birkebak, R.C. Appl. Optics 1966, 5, 1057.

5. Houk, R.S.; Montaser, A.; Fassel, V.A. Appl. Spectrosc. 1983, 37, 425.

6. Houk, R.S. Anal. Chem. 1986, 58, 97A.

7. Date, A.R.; Gray, A.L. Spectrochim. Acta, Part B 1983, 38B, 27.

8. Douglas, D.J.; Quan, E.S.K.; Smith, R.G. Spectrochim. Acta, Part B 1983, 38B, 39.

9. Douglas, D.J.; French, J.B. Spectrochim. Acta, Part B 1983, 41B, 197.

10. Gray, A.L. Spectrochim. Acta, Part B 1986, 41B, 151.

11. Alder, J.F.; Bombelka, R.M.; Kirkbright, G.F. Spectrochim. Acta, Part B 1980, 35B, 163.

12. Gray, A.L. J. Anal. Atomic Spectrom. 1983, 1, 247.

13. Gray, A.L.; Houk, R.S.; Williams, J.G. J. Anal. Atomic Spectrom. 1987, 2, 13.

14. Olivares, J.A.; Houk, R.S. Appl. Spectrosc. 1985, 39, 1070.

15. Crain, J.S.; Houk, R.S.; Eckels, D.E. Anal. Chem. 1989, 61, 606.

16. Kalnicky, D.J.; Fassel, V.A.; Kniseley, R.N. Appl. Spectrosc. **1977**, 31, 137.

17. Huang, L.-Q.; Jiang,S.-J.; Houk, R.S. Anal. Chem. **1987**, 59, 2316.

18. Horlick, G.; Tan, S.H.; Vaughan, M.A.; Rose, C.A. Spectrochim. Acta, Part B **1985**, 40B, 1555.

19. Vaughan, M.A.; Horlick, G.; Tan, S.H. J. Anal. Atomic Spectrom. **1987**, 2, 765.

20. de Galan, L.; Smith, R.; Winefordner, J.D. Spectrochim. Acta, Part B **1968**, 23B, 521.

21. Tamaki, S.; Kuroda, T. Spectrochim. Acta, Part B **1987**, 42B, 1105.

22. Caughlin, B.L.; Blades, M.W. Spectrochim. Acta, Part B **1985**, 40B, 987.

23. Caughlin, B.L.; Blades, M.W. Spectrochim. Acta, Part B **1985**, 40B, 1539.

24. Raeymakkers, B.; Broekart, J.A.C.; Leis, F. Spectrochim. Acta, Part B **1988**, 43B, 941.

25. Douglas, D.J.; French, J.B. J. Anal. Atomic Spectrom. **1988**, 3, 743.

26. Lovett, R.J. Spectrochim. Acta, Part B **1982**, 37B, 969.

27. Plantz, M.R.; Fritz, J.S.; Smith F.G.; Houk, R.S. Anal. Chem. **1989**, 61, 149.

28. Houk, R.S.; Schoer, J.K.; Crain, J.S. J. Anal. Atomic Spectrom. **1987**, 2, 283.

29. Scott, R.H.; Fassel, V.A.; Kniseley R.N.; Nixon, D.E. <u>Anal.</u>

<u>Chem</u>. **1974,** <u>46</u>, 75.

SUMMARY AND THOUGHTS FOR FUTURE RESEARCH

In addition to demonstrating the reliable application of mass spectrometry to the measurement of fundamental ICP properties, one objective of this dissertation was to describe some of the basic characteristics of an ICP ion source for mass spectrometry. In keeping with this goal, it was found that the ICP was the source of discrete, audio-frequency noise in the ICP mass-spectrometer signal, although the contribution of this type of noise to the overall instrumental stability was minor. Furthermore, observation of ionization energy-dependent matrix interferences indicated that these phenomena arose to some extent in the ICP itself, although changes in ion optical voltages and sampler-skimmer geometry also exerted an influence upon this effect.

An additional objective of this work was to suggest simple solutions to the analytical problems presented. In the case of ICP-MS noise, it was found that $1/f$ noise contributed strongly to the overall signal stability of the instrument. Several solutions to this problem were suggested. Improvements in the electronic stability of the mass spectrometer could be realized by incorporating power supplies in the instrument which have improved stability over those now in use. Such modifications may reduce the present $1/f$ noise problem by reducing transmission drift in the ion optics. However, such devices are unquestionably more expensive, and thus, in these times of budgetary conservation, more difficult to procure. A less expensive solution to the problem may rest with improved air circulation through the cabinet in which the electronic components are housed. If electronic drift is

thermal in nature, then, as the cabinet warms during operation, voltages applied to the various mass spectrometer components would change, thereby inducing signal drift. More efficient air circulation would be expected to eliminate such problems by closely controlling cabinet temperature. Such improvements have been noted for the Sciex ICP-MS instrument (56).

Unfortunately, solutions to the problem of matrix interference are not quite as simple to propose, for the most part due to the fact that the mechanisms by which matrix elements interfere with an analyte are not well-understood. For example, for the Sciex instrument, Gillson et al. (54) have proposed that the interference phenomena are entirely due to space-charge repulsions within the ion beam of the mass spectrometer, If this is so, then changes in ion optical design might attenuate or eliminate the interference. However, by changing sampler-skimmer geometry from the Sciex design, which yields mass-dependent interferences (24,28-35), to the geometry used in the present work, interferences become dependent on analyte ionization energy rather than on analyte mass. Gillson's mechanism fails to predict such a change, thus, it is incomplete. Models based on shifts in ionization reactions within the ICP itself (49,57) predict ionization energy-dependent interference, but fail to predict the extent to which a given amount of interferent will affect an analyte, or the mass-dependent interferences previously mentioned. It is obvious that further study of this effect at the fundamental level, i.e., using spectroscopic and electrical measurements within the plasma and supersonic expansion, will yield information crucial to the complete description of the problem and to

its eventual solution.

The question most frequently asked of a doctoral candidate is "What impact has your work had in your field?" This question is frequently difficult to answer. However, in the present case the answer to this important question lies not in the work itself, but in the apparatus used. For example, it is true that noise power spectra from an ICP-mass spectrometer had never been described, just as it is true that the variation, with ICP operating conditions, of ionization temperature measured by mass spectrometry had never agreed with those observed in prior optical temperature measurements. However, in the author's view, it is not these results, but the way in which they were obtained that will have a lasting impact upon ICP spectroscopy. This dissertation describes the first multidimensional ICP spectrometer, i.e., one capable of both optical and mass spectrometric measurement of the composition of an ICP. This capability permitted the unambiguous conclusion that the ICP was the source of discrete, audio-frequency noise in an ICP-mass spectrometer, just as it allowed the assignment of a reliable electron density to a given elemental ratio measurement at a specific set of ICP operating conditions. This advance in the information-gathering ability of ICP spectrometers, thus advancing the ability of these instruments to measure plasma properties, is the factor that sets this work apart from other ICP-mass spectrometry research. In this day of "hyphenated" analytical instrumentation, e.g., GC-MS and LC-MS, it seems that another device has been added to the list. The potential applications of this instrumentation in chemical analysis are wide-ranging, and only require an inquisitive mind to develop the applications.

ADDITIONAL LITERATURE CITED

1. Houk, R.S. Ph.D. Dissertation, Iowa State University, 1980.

2. Houk, R.S.; Fassel, V.A.; Flesch, G.D.; Svec, H.J.; Gray, A.L.; Taylor, C.E. Anal. Chem. 1980, 52, 2283.

3. Houk, R.S.; Fassel, V.A.; Svec, H.J. Dyn. Mass Spectrom. 1981, 6, 234.

4. Houk, R.S.; Svec, H.J.; Fassel, V.A. Appl. Spectrosc. 1981, 35, 380.

5. Houk, R.S.; Fassel, V.A.; Svec, H.J. Org. Mass Spectrom. 1982, 17, 240.

6. Houk, R.S.; Thompson, J.J. Am. Mineral. 1982, 67, 238.

7. Houk, R.S.; Montaser, A.; Fassel, V.A. Appl. Spectrosc. 1983, 37, 425.

8. Houk, R.S.; Thompson, J.J. Biomed. Mass Spectrom. 1983, 10, 107.

9. Douglas, D.J.; French, J.B. Anal. Chem. 1981, 53, 37.

10. Douglas, D.J.; Quan, E.S.K.; Smith, R.G. Spectrochim. Acta, Part B 1983, 38B, 39.

11. Douglas, D.J.; Rosenblatt; G.; Quan, E.S.K.; French, J.B. in "Symp. Proc., 6th Int. Symp. on Plasma Chem."; M.I. Boulos and R.J. Munz (Eds.); IUPAC, 1983, 2, 444.

12. Douglas, D.J.; Rosenblatt, G.; Quan, E.S.K. Quart. J. Plasma Chem. (Japan) 1983, 3, 1.

13. Douglas, D.J. Can. Res. 1983, 16, 55.

14. Gray, A.L.; Date, A.R. Dyn. Mass Spectrom. 1981, 6, 252.

15. Date, A.R.; Gray, A.L. Analyst **1981**, 106, 1255.

16. Date, A.R.; Gray, A.L. Analyst **1983**, 108, 159.

17. Date, A.R.; Gray, A.L. Spectrochim. Acta, Part B **1983**, 38B, 29.

18. Gray, A.L.; Date, A.R. Analyst **1983**, 108, 1033.

19. Gray, A.L.; Date, A.R. Int. J. Mass Spectrom. Ion Phys. **1983**, 46, 7.

20. Date, A.R.; Gray, A.L. Int. J. Mass Spectrom. Ion Phys. **1983**, 46, 357.

21. Doherty, W.; VanderVoet, A. Can. J. Spectrosc. **1985**, 30, 135.

22. Munro, S.; Ebdon, L.J.; McWeeney, D.J. J. Anal. Atomic Spectrom. **1986**, 1, 211.

23. Hutton, R.C. J. Anal. Atomic Spectrom. **1986**, 1, 259.

24. Beauchemin, D.; McLaren, J.W.; Berman, S.S. Spectrochim. Acta, Part B **1987**, 42B, 467.

25. McLaren, J.W.; Beauchemin, D.; Berman, S.S. Anal. Chem. **1987**, 59, 610.

26. Lichte, F.E.; Meier, A.L.; Crock, J.G. Anal. Chem. **1987**, 59, 1150.

27. Huang, L.-Q.; Jiang, S.-J.; Houk, R.S. Anal. Chem. **1987**, 59, 2316.

28. Longerich, H.; Strong, D.F.; Kantipuly, C.J. Can. J. Spectrosc. **1986**, 31, 111.

29. Palmeiri, M.D.; Fritz, J.S.; Thompson, J.J.; Houk, R.S. Anal. Chim. Acta **1986**, 184, 187.

30. Thompson, J.J.; Houk, R.S. Appl. Spectrosc. **1987**, 41, 801.

31. Tan, S.H.; Horlick, G. J. Anal. Atomic Spectrom. **1987**, 2, 745.

32. Gabarino, J.R.; Taylor, H.E. Anal. Chem. **1987**, 59, 1568.

33. Gregoire, D.C. Anal. Chem. **1987**, 59, 2479.

34. Longerich, H.P.; Fryer, B.J.; Strong, D.F. Spectrochim. Acta, Part B **1987**, 42B, 101.

35. Gregoire, D.C. Spectrochim. Acta, Part B **1987**, 42B, 895.

36. Serfass, R.E.; Thompson, J.J.; Houk, R.S. Anal. Chim. Acta **1986**, 188, 73.

37. Janghorbani, M.; Ting, B.T.G.; Fomon, S.J. Am. J. Hematol. **1986**, 21, 277.

38. Ting, B.T.G.; Janghorbani, M. Anal. Chem. **1986**, 58, 1334.

39. Serfass, R.E.; Lindberg, G.L.; Olivares, J.A.; Houk, R.S. Proc. Soc. Exp. Biol. Medicine **October 1987**, 186, 113.

40. Ting, B.T.G.; Janghorbani, M. Spectrochim. Acta, Part B **1987**, 42B, 21.

41. Sun, X.F.; Ting, B.T.G.; Zeisel, S.H.; Janghorbani, M. Analyst **187**, 112, 1223.

42. Janghorbani, M.; Davis, T.A.; Ting, B.T.G. Analyst **1988**, 113, 405.

43. Thompson, J.J; Houk, R.S. Anal. Chem. **1988**, 58, 2541.

44. VanLoon, J.C.; Alcock, L.R.; Pinchin, W.H.; French,J.B. Spectrosc. Lett. **1986**, 19, 1125.

45. Chong, N.S.; Houk, R.S. Appl. Spectrosc. **1987**, 41, 66.

46. McLeod, C.W. J. Anal. Atomic Spectrom. **1987**, 2, 549.

47. Dean, J.R.; Munro, S.; Ebdon, L.; Crews, H.M.; Massey, R.C. J. Anal. Atomic Spectrom. **1987**, 2, 607.

48. Koppenaal, D.W. ICP Info. Newsl. **1988**, 14, 267.

49. Olivares, J.A. Ph.D. Dissertation, Iowa State University, 1985.

50. Olivares, J.A.; Houk, R.S. Anal. Chem. **1985**, 57, 2674.

51. Douglas, D.J.; French, J.B. J. Anal. Atomic Spectrom. **1988**, 3, 743.

52. Campargue, R. J. Chem. Phys. **1984**, 88, 4466.

53. Beijerinck, H.C.W.; Van Gowen, R.J.F.; Kerestel, E.R.T.; Martens, J.F.M.; Van Vliembergen, E.J.W.; Smits, M.R.Th.; Kaashoek, G.H. Chem. Phys. **1985**, 96, 153.

54. Gillson, G.R.; Douglas, D.J.; Fulford, J.E.; Halligan, K.W.; Tanner, S.D. Anal. Chem. **1988**, 60, 1472.

55. Russ, G.P. III; Bazan, J. Spectrochim. Acta, Part B **1987**, 42B, 49.

56. Houk, R.S. Anal. Chem. **1986**, 58, 97A.

57. Olivares, J.A.; Houk, R.S. Anal. Chem. **1986**, 58, 20.

ACKNOWLEDGEMENTS

First and foremost, I want to give credit where credit is due.
None of this work would have been possible without the support,
guidance, and <u>tolerance</u> of Dr. R.S. Houk. It was he who put up with my
temperamental periods (when the rest of the group would not), my
obstinacy, and my occasional (frequent?) departures from the diligence
characteristic of the average graduate student in this chemistry
department. I am grateful for the academic freedom he allowed me, and
the guidance he gave me when I ran into stone walls in my work. I think
that this guidance was sometimes unintentional on his part, but then
again, one of the main functions of a research advisor (in my own,
albeit limited, view) is that of an "oracle" of useful information.
Professor Houk is most certainly that. I also appreciate the personal
relationship we have established during my tenure at Iowa State.
Whether it be softball, the Steelers, the Bucs, fishing, TV, movies, the
"Meaning of Life" or, less frequently, science, his door was always open
to me. Many of my peers envy my relationship with Dr. Houk, but
frankly, I feel that I simply got lucky in finding an advisor with whom
I have so much in common. I'm hopeful that our relationship will
continue after I leave Ames, both in a professional and personal sense.
Thanks Buddy.

I would like to acknowledge the support of my partners in crime,
the other members of the Houk group. Although my relations with many of
them were strained from time to time owing to clashing opinions (and
egos), I value their contributions to my development as a scientist, as

well as the lessons they've taught me with regards to "working and playing" well with others. The idea of keeping my mouth shut when I don't agree with someone was quite foreign to me when I came here (and still is to some degree), but, in my time here, I've seen that there are times to chime in, as well as times to keep one's trap shut. That lesson will remain with me for a long time to come.

The contributions of the Ames Laboratory staff cannot be underestimated. My machinist friends (Harry Amenson, Tom Johnson, and Dean Westberg) made me re-learn everything I had forgotten about working and shaping metals. This skill has been invaluable to my work in graduate school (especially when the "Valiant" was reconstructed), and will undoubtedly be valuable up to the time I end my career. To them I owe a debt of professional thanks which really cannot be adequately set on paper. The generous contribution of plasma equipment by the Perkin-Elmer Corporation is gratefully acknowledged, as is the loan of a spectrum analyzer by Richard Hendrickson of the Iowa State University Department of Nuclear Engineering. Finally, I want to acknowledge the contributions of Dave Eckels and Royce Winge to my work on noise measurements. Dave's ability to take the theory of noise production and put it into physical perspective never failed to amaze me, and Royce's wealth of helpful suggestions and camera work was invaluable during the course of the noise studies.

Without friends, a man can certainly attain his goals, but he'll spend a lot of lonely Friday and Saturday nights in the process, and ultimately, he'll have no one with whom he can share his successes. Fortunately, I've been given a circle of friends with whom I have shared

a great deal, and to whom I owe a great deal. My fishing/hunting buddies, Dave (the Georgia Peach) Sanders, Steve J., Kevin D., Kevin C., Jeff, and yes, even Glenn, have not allowed me to forget what enjoying the outdoors is all about. The presence of Diane (the Creature), the Marys, Deb, Les, and Chris have frequently reminded me that my barbaric tendencies are not suitable for mixed company, but they accepted me nonetheless. Last (but not least), Thom, Clark, and more recently, Dave Mac and Bill, were always there when beer was indicated by the circumstances, and even on several occasions when it was not. To all of you that I have mentioned, I thank you for keeping me sane, but not always in balance. To those I may have forgotten, I apologize and thank you as well. I will miss you, one and all.

Finally, I owe my greatest debt to my family. I have never appreciated or entirely understood the reasons why my father pushed me toward college, but I think he wanted me to realize that my life could be better than the golf course or the mills would ever allow. I think that he would be proud of me now, and now, more than ever before, I mourn his loss. I wish I could share this achievement with him. However, my surviving family (grandpap, mom, and Bruce) have always been supportive of my work, and have encouraged me to go on, even when things seemed darkest. My time in graduate school would have been far more miserable without the reassurance of my mother during our weekly phone calls, and without the love and support I received from my family during my visits home (even the unscheduled ones!). Mom, this is your dissertation as well as my own. Congratulations.

APPENDIX.   COMPUTER PROGRAMS

Electron Density Calculation

An interactive computer program called NECALC.FOR was written to perform the calculation of electron density in the observed region of the ICP. This program, shown in Table A-1, was written in the ANSI FORTRAN/77 computer language. The only input variable for this program was the uncorrected half-width of the H_β emission line at 486.13 nm. The reduced Stark half-width parameter was calculated at an arbitrary gas temperature of 5000 K.

Ionization Temperature Calculation

Interactive computer programs called TCALCAS.FOR and TCALCSB.FOR were written to perform ionization temperature calculations for As and Sb respectively. These programs, shown in Table A-2, were written in the ANSI FORTRAN/77 computer language. In both programs, the input variables were elemental ratio (either As^+/Ga^+ or Sb^+/In^+), electron density (from NECALC.FOR) and an initial ionization temperature, usually 7000 K.

Table A-1. FORTRAN Computer Program NECALC.FOR

```
*                 NECALC
*                 WRITTEN BY J.CRAIN, 1/9/89
*
*
*     This program is designed to calculate ICP electron density
*     using experimentally measured half widths of the H I 486.13 nm
*     emission line.  n_e is calculated iteratively using the method
*     described in Kalnicky's thesis.
*
* Variables:
*     ALPHA = reduced Stark half-width parameter
*     EDENS = electron density
*     DLAMB = FWHM of H I emission
*
* Functions:
*     EDENS = 7.9653E12*(DLAMB/ALPHA)**1.5
*
      IMPLICIT REAL*4 (A-H,O-Z), INTEGER*4 (I-N)
      WRITE (6,*) ' '
      WRITE (6,*) '                 WELCOME TO NECALC'
      WRITE (6,*) ' '
      WRITE (6,*) 'This program calculates ICP electron density based'
      WRITE (6,*) 'on Stark Broadening of the H I 486.13 nm emission'
      WRITE (6,*) 'line.  The calculation is made at an arbitrary gas'
      WRITE (6,*) 'temperature of 5000 K using the method described in'
      WRITE (6,*) 'Appl. Spectrosc. 1977, 31, 137-150.'
    1 WRITE (6,*) ' '
      WRITE (6,*) 'INPUT THE FWHM (in Angstroms) OF H I 486.13 nm.'
      READ (5,*) DLAMB
*
      DLAMB = 0.6*DLAMB
*
* THE ABOVE FUDGE FACTOR CORRECTS FOR THE DIFFERENT SLIT WIDTHS USED
* IN KALNICKY'S EXPERIMENTS AND MY OWN. OTHERWISE, THE MONOCHROMATOR
* AND OTHER THINGS WERE THE SAME.
*
      ALPHA0 = 0.07539
      EDENS0 = 7.9653E12*(DLAMB/ALPHA0)**1.5
*
      DO 99 I=1,100
         IF (EDENS0 .GE. 1.0E15 .AND. EDENS0 .LE. 3.162E15) GOTO 11
         IF (EDENS0 .GE. 3.162E14 .AND. EDENS0 .LT. 1.0E15) GOTO 21
         GOTO 100
   11    ALPHA=7.70505E-02-(1.6605E-03*(EDENS0/1.0E15))
         EDENS=7.9653E12*(DLAMB/ALPHA)**1.5
         ERAT=EDENS/EDENS0
         GOTO 31
   21    ALPHA=9.52935E-02-(1.99035E-03*(EDENS0/1.0E14))
```

Table A-1.   (continued)

```
        EDENS=7.9653E12*(DLAMB/ALPHA)**1.5
        ERAT=EDENS/EDENS0
 31     IF (ERAT .GE. 0.999 .AND. ERAT .LE. 1.001) GOTO 101
        EDENS0=EDENS
 99  CONTINUE
*
     WRITE (6,*) ' NO CONVERGENCE AFTER 100 ITERATIONS.'
     GOTO 102
100  WRITE (6,*) 'CALCULATION OUT OF PROGRAMMED LIMITS.'
     WRITE (6,*) 'CHECK SOURCE CODE FOR LIMITS; MODIFY IF NEEDED.'
     GOTO 102
101  WRITE (6,*) 'AFTER ',I,' ITERATIONS'
     WRITE (6,*) 'e Density is ', EDENS
     WRITE (6,*) 'Reduced Half-width param. is', ALPHA
102  WRITE (6,*) ' '
     WRITE (6,*) 'DO YOU WANT TO GO AGAIN? YES=1, NO=ANYTHING ELSE'
     READ (5,*) ICHOOSE
     IF (ICHOOSE .EQ. 1) GOTO 1
     WRITE (6,*) 'Thank you for using NECALC. Have a nice day'
     STOP
     END
```

Table A-2. FORTRAN Computer Programs TCALCAS.FOR and TCALCSB.FOR

```
*               TCALCAS
*               WRITTEN BY J.CRAIN, 11/7/88
*               LAST REVISED 1/18/89
*
*    This program is designed to calculate ICP ionization temperature
*    using experimentally measured degrees of ionization and electron
*    density for As and Ga.  Tion is calculated iteratively by solving
*    the Saha-Eggert equation for the given values of α and n_e using
*    the Newton-Raphson method.
*
* Variables:
*    ALPHA = degree of ionization
*    EDENS = electron density
*    TOLD,TNEW = ionization temperatures
*    ZRAT = ion/atom partition function ratio
*
* Constants:
*    ENERGY = ionization energy for M
*    BOLTZK = Boltzmann's constant = 8.62E-05 eV/K
*
* Functions:
*    FACTOR = 2.08E-16*ALPHA*EDENS/(ZRAT*(1-ALPHA))
*    FUNCT = 1.5*LN(TNEW)-ENERGY/BOLTZK/TNEW-LN(FACTOR)
*    DFUNCT = 1.5/TNEW+ENERGY/BOLTZK/(TNEW**2)
*    TNEW = TOLD - FUNCT/DFUNCT
*
      IMPLICIT REAL*4 (A-H,O-Z), INTEGER*4 (I-N)
      WRITE (6,*) 'Welcome to TCALCAS'
      WRITE (6,*) 'Calculation routine to obtain Tion from As/Ga'
      WRITE (6,*) ' '
      WRITE (6,*) 'WHAT Tion (in K) DO YOU WANT TO START AT?'
      READ (5,*) TNEW
   1  WRITE (6,*) 'INPUT THE EXPERIMENTAL As/Ga RATIO'
      READ (5,*) RATION
      WRITE (6,*) 'INPUT THE EXPERIMENTAL ELECTRON DENSITY'
      READ (5,*) EDENS
*
      ASBOLT=9.81/8.62E-5
      GABOLT=5.999/8.62E-5
      ERAT=EDENS/4.8125E15
*
      DO 99 I=1,100
         REDT=TNEW/1000.
         IF (TNEW .GE. 7000.)GOTO 11
*
         ZASI=4.2641-(0.27507*REDT)+(7.5632E-2*REDT**2)-
     1(2.3876E-3*REDT**3)
```

Table A-2. (continued)

```
        ZASII=(2.284*REDT)-0.25384-(0.33383*REDT**2)
   2+(3.0408E-02*REDT**3)-(1.1609E-3*REDT**4)
        ZGAI=1.7931+(1.9338*REDT)-(0.4643*REDT**2)+(5.4876E-2*REDT**3)-
   3(2.5054E-3*REDT**4)
        GOTO 12
*
  11    ZASI=(2.5553E-2*REDT**2)+(6.7896E-2*REDT)+3.4981
        ZASII=(1.064*REDT)+1.6134-(4.1618E-2*REDT**2)
        ZGAI=2.3711+(0.84502*REDT)-(5.9079E-2*REDT**2)
*
  12    GAFAC=EXP(GABOLT/TNEW)
        GALF=1./((ERAT*ZGAI*GAFAC/TNEW**1.5)+1.0)
        ALPHA=RATION*GALF
        WRITE (6,*)GALF,ALPHA
*

        FACTOR=ALPHA*ERAT*ZASI/ZASII/(1.-ALPHA)
        FACLOG=LOG(FACTOR)
        FUNCT=1.5*LOG(TNEW)-(ASBOLT/TNEW)-FACLOG
        DFUNCT=1.5/TNEW+(ASBOLT/(TNEW**2))
        TOLD=TNEW
        TNEW=TOLD-FUNCT/DFUNCT
        TRAT=TNEW/TOLD
        IF (TRAT .GE. 0.9999 .AND. TRAT .LE. 1.0001) GOTO 101
  99 CONTINUE
*
     WRITE (6,*) ' NO CONVERGENCE AFTER 100 ITERATIONS. TRY A NEW T'
     WRITE (6,*) ' '
     GOTO 1
 101 WRITE (6,*) ' '
     WRITE (6,*) 'After ',I,' Iterations'
     WRITE (6,*) 'Tion is ', TNEW
     WRITE (6,*) 'Deg. of Ioniz.(As) is',ALPHA
 102 WRITE (6,*) ' '
     WRITE (6,*) 'DO YOU WANT TO GO AGAIN? YES=1, NO=ANYTHING ELSE'
     READ (5,*) ICHOOSE
     IF (ICHOOSE .NE. 1) GOTO 103
     GOTO 1
 103 WRITE (6,*) ' '
     WRITE (6,*) 'Thank you for using TCALCAS. Have a nice day'
     STOP
     END
```

Table A-2.   (continued)

```
*               TCALCSB
*               WRITTEN BY J.CRAIN, 11/7/88
*               LAST REVISED 1/18/89
*
*     This program is designed to calculate ICP ionization temperature
*     using experimentally measured degrees of ionization and electron
*     density for Sb and In.  Tion is calculated iteratively by solving
*     the Saha-Eggert equation for the given values of α and n_e using
*     the Newton-Raphson method.
*
* Variables:
*     ALPHA = degree of ionization
*     EDENS = electron density
*     TOLD,TNEW = ionization temperatures
*     ZRAT = ion/atom partition function ratio
*
* Constants:
*     ENERGY = ionization energy for M
*     BOLTZK = Boltzmann's constant = 8.62E-05 eV/K
*
* Functions:
*     FACTOR = 2.08E-16*ALPHA*EDENS/(ZRAT*(1-ALPHA))
*     FUNCT = 1.5*LN(TNEW)-ENERGY/BOLTZK/TNEW-LN(FACTOR)
*     DFUNCT = 1.5/TNEW+ENERGY/BOLTZK/(TNEW**2)
*     TNEW = TOLD - FUNCT/DFUNCT
*
      IMPLICIT REAL*4 (A-H,O-Z), INTEGER*4 (I-N)
      WRITE (6,*) 'Welcome to TCALCSB'
      WRITE (6,*) 'Calculation routine to obtain Tion from Sb/In'
      WRITE (6,*) ' '
      WRITE (6,*) 'WHAT Tion (in K) DO YOU WANT TO START AT?'
      READ (5,*) TNEW
   1  WRITE (6,*) 'INPUT THE EXPERIMENTAL Sb/In RATIO'
      READ (5,*) RATION
      WRITE (6,*) 'INPUT THE EXPERIMENTAL ELECTRON DENSITY'
      READ (5,*) EDENS
*
      SBBOLT=8.641/8.62E-5
      BOLTIN=5.786/8.62E-5
      ERAT=EDENS/4.8125E15
*
      DO 99 I=1,100
         RDT=TNEW/1000.
*
         ZSBI=4.3114-(0.35581*RDT)+(0.11172*RDT**2)-
     1(4.4909E-3*RDT**3)-(4.4389E-5*RDT**4)
         ZSBII=0.91346-(0.15093*RDT)+(0.27036*RDT**2)
     2-(3.7073E-02*RDT**3)+(1.7249E-3*RDT**4)
```

Table A-2.   (continued)

```
*
        IF (TNEW .GE. 7000) GOTO 11
*
        ZINI=1.0731+(1.1097*RDT)-(0.13211*RDT**2)+(6.3919E-3*RDT**3)
        ZINII=1.0
        GOTO 12
*
   11   ZINI=13.381-(2.6861*RDT)+(0.20733*RDT**2)
        ZINII=1.0547-(1.8883E-2*RDT)+(1.5042E-3*RDT**2)
*
   12   FACIN=EXP(BOLTIN/TNEW)
        ALFIN=1./((ERAT*ZINI*FACIN/ZINII/TNEW**1.5)+1.0)
        ALPHA=RATION*ALFIN
        WRITE (6,*)ALFIN,ALPHA
*
        FACTOR=ALPHA*ERAT*ZSBI/ZSBII/(1.-ALPHA)
        FACLOG=LOG(FACTOR)
        FUNCT=1.5*LOG(TNEW)-(SBBOLT/TNEW)-FACLOG
        DFUNCT=1.5/TNEW+(SBBOLT/(TNEW**2))
        TOLD=TNEW
        TNEW=TOLD-FUNCT/DFUNCT
        TRAT=TNEW/TOLD
        IF (TRAT .GE. 0.9999 .AND. TRAT .LE. 1.0001) GOTO 101
   99 CONTINUE
*
      WRITE (6,*) ' NO CONVERGENCE AFTER 100 ITERATIONS. TRY A NEW T'
      WRITE (6,*) ' '
      GOTO 1
  101 WRITE (6,*) ' '
      WRITE (6,*) 'After ',I,' Iterations'
      WRITE (6,*) 'Tion is ', TNEW
      WRITE (6,*) 'Deg. of Ioniz.(Sb) is',ALPHA
  102 WRITE (6,*) ' '
      WRITE (6,*) 'DO YOU WANT TO GO AGAIN? YES=1, NO=ANYTHING ELSE'
      READ (5,*) ICHOOSE
      IF (ICHOOSE .NE. 1) GOTO 103
      GOTO 1
  103 WRITE (6,*) ' '
      WRITE (6,*) 'Thank you for using TCALCSB. Have a nice day'
      STOP
      END
```